foxQ2 has a key role in anterior head and central brain patterning in insects

Peter Kitzmann[1], Matthias Weißkopf[2], Magdalena Ines Schacht[1], Gregor Bucher[1]

[1] Department of Evolutionary Developmental Genetics, GZMB, Universität Göttingen, Justus von Liebig Weg 11, 37077 Göttingen

[2] Department of Biology, Division of Developmental Biology, Friedrich-Alexander-University of Erlangen-Nürnberg, Erlangen, Germany

The authors declare no competing interests.

Funding:

Deutsche Forschungsgemeinschaft (DFG)

Göttingen Graduate School for Neurosciences, Biophysics, and Molecular Biosciences (GGNB)

Abstract

Anterior patterning of animals is based on a set of highly conserved transcription factors but the interactions within the protostome anterior gene regulatory network (aGRN) remain enigmatic. Here, we identify the *foxQ2* ortholog of the red flour beetle *Tribolium castaneum* as novel upstream component of the aGRN. It is required for the development of the labrum and higher order brain structures, namely the central complex and the mushroom bodies. We reveal *Tc-foxQ2* interactions by RNAi and heat shock-mediated misexpression. Surprisingly, *Tc-foxQ2* and *Tc-six3* mutually activate each other forming a novel regulatory module at the top of the aGRN. Comparisons of our results with those of sea urchins and cnidarians suggest that *foxQ2* has acquired more upstream functions in the aGRN during protostome evolution. Our findings expand the knowledge on *foxQ2* gene function to include essential roles in epidermal development and central brain patterning.

Author summary

The development of the anterior most part of any animal embryo – for instance the brain of vertebrates and the anterior head of insects – depends on a very similar set of genes present in all animals. This is true for the two major lineages of bilaterian animals, the deuterostomes (including sea urchin and humans) and protostomes (including annelids and insects) and the cnidarians (e.g. the sea anemone), which are representatives of more ancient animals. However, the interaction of these genes has been studied in deuterostomes and cnidarians but not in protostomes. Here, we present the first study of the function of the gene *foxQ2* in protostomes. We found that the gene acts at the top level of the genetic network and when its function is knocked down, the labrum (a part of the head) and higher order brain centers do not develop. This is in contrast to the other animal groups where *foxQ2* appears to play a less central role. We conclude that *foxQ2* has acquired additional functions in the course of evolution of protostomes.

Introduction

Anterior patterning in bilaterian animals is based on a set of highly conserved transcription factors like *orthodenticle*/*otx*, *empty spiracles*/*emx*, *eyeless*/*Pax6* and other genes, which have comparable expression and function from flies to mice (Hirth et al., 1995; Leuzinger et al., 1998; Quiring et al., 1994; Simeone et al., 1992). Likewise, canonical Wnt signaling needs to be repressed in order to allow anterior pattern formation in most tested animals with *Drosophila* being a notable exception (Fu et al., 2012; Martin and Kimelman, 2009; Petersen and Reddien, 2009). Since recently, additional genes have been studied, which are expressed anterior to the *orthodenticle/otx* region at the anterior pole of embryos of all major clades of Bilateria and their sister group, the Cnidaria. These data suggested that a distinct but highly conserved anterior gene regulatory network (aGRN) governs anterior-most patterning (Lowe et al., 2003; Marlow et al., 2014; Posnien et al., 2011b; Sinigaglia et al., 2013; Steinmetz et al., 2010; Yaguchi et al., 2008). This region gives rise to the apical organ in sea urchins, annelids and hemichordates and other structures. Most of the respective orthologs were shown to be expressed in the vertebrate anterior neural plate and the anterior insect head as well (Posnien et al., 2011b) although it remains disputed what tissue-if any-is homologous to the apical organ in these species (Hunnekuhl and Akam, 2014; Marlow et al., 2014; Santagata et al., 2012; Sinigaglia et al., 2013; Telford et al., 2008). Detailed interactions of this aGRN were determined only in a few model systems (Range and Wei, 2016; Sinigaglia et al., 2013; Yaguchi et al., 2008).

The aGRN of sea urchins as representative of deuterostomes is best studied in *Strongylocentrotus purpuratus* and *Hemicentrotus pulcherrimus*. Here, *six3* (*sine oculis homeobox homolog 3/optix*) is the most upstream regulator, which is initially co-expressed with *foxQ2*. Both genes are restricted to the anterior pole by repression by posterior Wnt signaling (Range and Wei, 2016; Wei et al., 2009;

Yaguchi et al., 2008). *six3* in turn is able to repress Wnt signaling (Wei et al., 2009) and to activate a large number of genes including *rx, nk2.1* and *foxQ2* (Wei et al., 2009). Subsequently, *foxQ2* represses *six3* but activates *nk2.1* expression at the anterior-most tip. In this tissue freed of *six3* expression *foxQ2* is responsible for establishing a signaling center involved in the differentiation of the apical organ (Range and Wei, 2016). In addition, *foxQ2* expression is activated by nodal signaling (Yaguchi et al., 2016). *six3* knockdown leads to a strong morphological phenotype including change of embryonic epidermal shape and loss of neural cells (Wei et al., 2009). In *foxQ2* knockdown, in contrast, an epidermal phenotype other than animal plate thickening was not observed (Yaguchi et al., 2008) but *foxQ2* appears to be essential for the specification of neural cell types (Yaguchi et al., 2008; Yaguchi et al., 2012; Yaguchi et al., 2016).

Nematostella vectensis (Cnidaria) represents the sister group to bilaterian animals (Sinigaglia et al., 2013). Here, both *Nv-six3* and *Nv-foxQ2* are initially activated by Wnt/β-catenin signaling, while at later stages there seems to be an antagonism between Wnt/β-catenin signaling and *Nv-six3* (Leclère et al., 2016). *Nv-six3* activates *Nv-foxQ2* and several other genes of the aGRN (Marlow et al., 2013; Sinigaglia et al., 2013). Like in the sea urchin, knockdown of *Nv-six3* leads to strong morphological defects including loss of the apical organ while *Nv-foxQ2* knockdown does not affect the morphology of the embryo but the apical organ is reduced (Sinigaglia et al., 2013). In contrast to sea urchin *Nv-foxQ2* does not appear to regulate *Nv-six3*. The repression of *six3* and *foxQ2* by Wnt signaling has been shown for a hemichordate (deuterostome) (Darras et al., 2011; Fritzenwanker et al., 2014) and for *foxQ2* in a hydrozoan (cnidarian) (Momose et al., 2008). Neither sea urchins nor cnidarians possess a highly centralized nervous systemsuch that a function of *foxQ2* in brain development could not be tested.

Within protostomes, the expression of aGRN genes has been studied extensively in postembryonic stages of the annelid *Platynereis dumerilii* (Lophotrochozoa). However, the only functional interaction tested was the repression of *Pd-six3* and *Pd-foxQ2* by Wnt signaling, which was activated

by pharmacological activation (Marlow et al., 2014). Within arthropods (Ecdysozoa) the red flour beetle *Tribolium castaneum* has become the main model system for studying anterior patterning (Posnien et al., 2010), because head development is more representative for insects than the involuted head of *Drosophila*. Indeed, the anterior morphogen *bicoid* is present only in some dipterans while the canonical anterior repression of Wnt signaling is observed in *Tribolium* only (Brown et al., 2001; Stauber et al., 1999, Fu et al., 2012). Neither terminal Torso signaling nor the terminal gap gene *huckebein* have an influence on head formation in *Tribolium* (Schoppmeier and Schröder, 2005; Kittelmann et al., 2013). Apart from a region with similarity to vertebrate neural plate patterning there is also a largely non-neural anterior median region (AMR) patterned by other genes (Kittelmann et al., 2013; Posnien et al., 2011b). Interestingly, *Tc-six3* is a central regulator of anterior head and brain patterning, which is repressing *Tc-wg* expression among other genes but is not regulating *Tc-rx* and *Tc-nk2.1* (Posnien et al., 2011b).

In an ongoing genome-wide RNAi screen in *Tribolium* (iBeetle screen) (Dönitz et al., 2015; Schmitt-Engel et al., 2015) a head phenotype similar to the one of *Tc-six3* was induced by the dsRNA fragment *iB_03837*. The targeted gene was the *Tribolium* ortholog of FoxQ2 (*Tc-foxQ2*), which encodes a Forkhead transcription factor. All members of this family share the Forkhead DNA-binding domain and they are involved in development and disease (Benayoun et al., 2011). While being highly conserved among animals, this gene was lost from placental mammals (Mazet et al., 2003; Yu et al., 2008). Within arthropods, anterior expression was described for the *Drosophila* ortholog *fd102C* (*CG11152*) (Lee and Frasch, 2004) and *Strigamia maritima* (myriapod) *foxQ2* (Hunnekuhl and Akam, 2014). However, the function of this gene has not been studied in any protostome so far.

We studied expression and function of *Tc-foxQ2* by RNAi and heat shock-mediated misexpression and found that *Tc-foxQ2* has a much more central role in the insect aGRN compared to sea urchin and cnidarians. Surprisingly, *Tc-foxQ2* and *Tc-six3* form a regulatory module with mutual activation contrasting the clear upstream role of *six3* in the other species. Another difference is that *Tc-foxQ2*

knockdown led to a strong epidermal phenotype. Further, we found a novel role of *Tc-foxQ2* in CNS patterning. Specifically, it was required for the development of the mushroom bodies (MB) and the central complex (CX), both of which are higher order processing centers of the insect brain (Heisenberg, 2003; Pfeiffer and Homberg, 2014). Finally, we present the most comprehensive aGRN available for protostomes.

Results

Tc-foxQ2 - a novel player in anterior head development of *Tribolium*

In the iBeetle screen, injection of the dsRNA fragment *iB_03837* led to first instar larval cuticles with reduced or absent labrum (cyan area in Fig. 1) with high penetrance (Dönitz et al., 2015; Schmitt-Engel et al., 2015) (Fig. 1A). The targeted gene was *TC004761* (Tcas_OGS 3.0), which ourrevealed as the sole *Tribolium* ortholog of FoxQ2 (Tc-FoxQ2) (Fig. S1). Quantitative analyses of parental RNAi experiments with two non-overlapping dsRNA fragments (*Tc-foxQ2*$^{RNAi\_a}$; *Tc-foxQ2*$^{RNAi\_b}$; 1.5 µg/µl) (Fig. 1A,B; Tables S1-4) in two different genetic backgrounds (Fig. S2; Tables S3-6) revealed the same morphological phenotype arguing against off-target effects or strong influence of the genetic background (Kitzmann et al., 2013). The proportions of eggs without cuticles or with cuticle remnants (*strong defects*) were within in the range observed in wild-type (WT) (van der Zee et al., 2005). Weak *Tc-foxQ2* RNAi phenotypes showed a labrum reduced in size and loss of one or both labral setae (Fig. 1E,F; yellow dots). Intermediate phenotypes were marked by a reduced labrum and loss of one or both anterior vertex triplet setae (Fig. 1E,G; red dots) indicating additional deletions of the head capsule. In strong phenotypes, the labrum was strongly reduced or deleted along with several setae marking the anterior head and/or the labrum (Fig. 1H). No other specific L1 cuticle

phenotypes were detected. We tested higher dsRNA concentrations (2 µg/µl and 3.1 µg/µl; data not shown) as well as double RNAi using both dsRNA fragments together (1.5 µg/µl each; data not shown). None of these variations resulted in a stronger cuticle phenotype. Taken together, *Tc-foxQ2* is required for epidermal patterning of anterior head structures. Interestingly, the RNAi phenotype was similar to the one of *Tc-six3* although somewhat weaker and less penetrant (Posnien et al., 2011b).

Increased apoptosis in *Tc-foxQ2* RNAi

The labrum is an appendage-like structure (Posnien et al., 2009a) and its outgrowth requires cell proliferation regulated by *Tc-serrate (Tc-ser)* (Siemanowski et al., 2015). We asked when the size of the labrum decreased after *Tc-foxQ2* RNAi and whether cell proliferation or cell death were involved. We found that the labral buds in *Tc-foxQ2*^{RNAi} embryos were decreased and fused from fully elongated germ band stages onwards (Fig. 2Aa`-d`). We found no regulation of *Tc-ser* by *Tc-foxQ2* (see below). Next, we quantified apoptosis in embryos (6-26 h after egg laying (AEL); Table S7) using an antibody detecting cleaved death caspase-1 (Dcp-1) (Florentin and Arama, 2012). We quantified apoptotic cells in the labral region (region 1 in Fig. 2B) and a control region (region 3). Fully elongated germ bands showed a six times increased number of apoptotic cells after *Tc-foxQ2* RNAi (p=0.00041, n=15; Fig. 2C) coinciding with the stage of morphological reduction. Hence, *Tc-foxQ2* prevents apoptosis in the growing labrum.

Tc-foxQ2 is required for brain development

The phenotypic similarity to *Tc-six3*^{RNAi} embryos (Posnien et al., 2011b) and the expression of *Tc-foxQ2* in neuroectodermal tissue (see below) prompted us to check for brain phenotypes. We performed parental RNAi in the background of the *brainy* line, which marks glia by ECFP (black signal in Fig. 3A-C) (Koniszewski et al., 2016). In the weakest phenotypes, the medial lobes of the MBs were reduced and appeared to be medially fused (Fig. 3, compare empty arrowheads in A with B; MBs marked in magenta). Further, the central body (CB; part of the CX) was shortened (Fig. 3B, CB marked in yellow) and the brain hemispheres were slightly fused (Fig. 3, compare cyan arrowheads in B with A). In stronger phenotypes, the CB was clearly reduced in size and the MBs were not detectable anymore. Further, the brain hemispheres appeared fused at the midline (Fig. 3C). We performed RNAi in the background of the transgenic *MB-green* line which marks MBs by EGFP (Koniszewski et al., 2016) (magenta-enframed black signal in Fig. 3D-H). We observed a similar range of MB body phenotypes. In addition to fused MBs, we found misarranged MBs that had lost their medial contact (Fig. 3F,G, light green arrowheads), interdigitated MBs (Fig. 3G), and highly reduced or even absent MBs (Fig. 3H). Noteworthy, the strength of epidermal and neural phenotypes correlated. Larvae with weak neural defects showed a decreased labrum, while strong neural phenotypes correlated with lack of the entire labrum. Taken together, we found *Tc-foxQ2* to be required for brain formation with the MBs, the CB, and the midline being strongly affected. Again, these defects are similar to those reported for *Tc-six3* loss-of-function (Posnien et al., 2011b).

Dynamic expression of *Tc-foxQ2* in the anterior head

The expression of *Tc-foxQ2* started in two domains at the anterior terminus of the germ rudiment (Fig. 4A,B). During elongation, the two domains approach each other due to morphological movements (Fig. 4C-E). At late elongating germ band stages, the domains split into several subdomains in the AMR and the labrum anlagen (empty arrowhead in Fig. 4F,H) and domains lateral

to the stomodeum (empty arrow in Fig. 4G,I). Besides, there are domains in the neuroectoderm (e.g. white arrow in Fig. 4F,L; see approximate fate map in Fig. S3). Very weak staining in the ocular region was detected with the tyramide signal amplification (TSA) system (Fig. 4K). These data are comparable to the anterior expression of *foxQ2* orthologs in other animals and consistent with the phenotype in *Tribolium*.

We mapped the expression of *Tc-foxQ2* relative to other genes of the aGRN by double in situ hybridization in WT embryos. Expression overlaps are marked with dashed lines in Figs 5 and S4. First we tested for genes that interact with *foxQ2* in other species or are required for labrum formation (Coulcher and Telford, 2012; Economou and Telford, 2009; Kittelmann et al., 2013; Posnien et al., 2009a; Posnien et al., 2011b). We found no overlap with *Tc-wingless/wnt1* (*Tc-wg*) expression until retraction, where the emerging stomodeal *Tc-wg* domain overlapped with *Tc-foxQ2* expression (Fig. 5A). In contrast, we found complete overlap with *Tc-six3* expression at early embryonic stages (Fig. $5B_1$), which developed into a mutually exclusive expression at intermediate elongating germ bands (Fig. $5B_3$). Afterwards, these genes remained expressed mutually exclusive apart from a small anterior median neuroectodermal region (lateral area marked in Fig. $5B_{4-7}$) and the labrum anlagen (median area marked in Fig. $5B_{6-7}$). These data are in agreement with the interactions described for sea urchin where *six3* initially activates *foxQ2* while at later stages *six3* gets repressed by *foxQ2* (see introduction). The later coexistence of mutually exclusive and co-expression domains along with the many different expression domains of *Tc-foxQ2* indicate a complex and region specific regulation. Early co-expression developing into partially overlapping expression patterns was observed for both *Tc-cap´n´collar* (*Tc-cnc*) and *Tc-scarecrow* (*Tc- scro/nk2.1*) (Fig. 5C-D). For *Tc-crocodile* (*Tc-croc*) a small overlap was observed, which remained throughout development (Fig. 5E).

Next we studied genes that based on expression and function were supposed to be downstream components of the aGRN. *Tc-retinal homeobox* (*Tc-rx*) was expressed in a largely non-overlapping pattern apart from small domains in labrum and neuroectoderm at late stages (Fig. S4A). *Tc-chx* and *Tc-ser* start expression largely overlapping with *Tc-foxQ2* but later resolve to mainly non-overlapping patterns (Fig. S4B,E). *Tc-forkhead (Tc-fkh/foxA)* expression was essentially non-overlapping (Fig. S4C). *Tc-six4* marks a region with molecular similarity to the vertebrate placodes (Posnien et al., 2011a). No co-expression was observed until late stages where a small domain expresses both genes (Fig. S4D). In summary, *Tc-foxQ2* expression indicated a central and dynamic role in the aGRN.

Tc-foxQ2 is required for *Tc-six3* expression and is repressed by Wnt signaling

We first tested the interactions of *foxQ2* known from other species. *Tc-foxQ2* was virtually absent in *Tc-six3* RNAi embryos (Fig. $6C_{1\text{-}3}$) indicating a conserved role of *Tc-six3* in *Tc-foxQ2* activation. Only later stages showed some residual *Tc-foxQ2* expression in the stomodeal region (not shown). Unexpectedly, *Tc-six3* expression was strongly reduced in *Tc-foxQ2*^{RNAi} germ rudiments (compare Fig. $6B_1$ with D_1), which contrasts findings in cnidarians and sea urchins. At later stages, medial *Tc-six3* expression emerged (Fig. $6D_2$) and developed a similar shape and intensity as in WT (Fig. $6D_3$). However, the lateral neuroectodermal domains remained strongly reduced or even absent (Fig. $6D_2$,D_3; empty arrowheads). Efficient knock-down of *Tc-foxQ2* by RNAi was shown by in situ hybridization and RT-qPCR (Fig. S5 and S6). The activation of *Tc-six3* by *Tc-foxQ2* at early stages was confirmed by RT-qPCR experiments (Fig. S6).

At early embryonic stages, *Tc-wg* expression was not altered in *Tc-foxQ2*^{RNAi} (not shown). Likewise, inhibition of canonical Wnt signaling by *Tc-arr* RNAi did not alter *Tc-foxQ2* expression at early stages (Fig. 6E$_{1/2}$). Later, the neuroectodermal *Tc-foxQ2* expression domains were expanded (Fig. 6E$_3$; empty arrowhead), whereas the anterior labral *Tc-foxQ2* expression domain was lost (Fig. 6E$_3$; arrowhead). The *Tc-six3* expression domains were expanded in *Tc-arr*^{RNAi} germ rudiments covering the anterior region (Fig. 6F$_1$). Later, the neuroectodermal *Tc-six3* expression domains were strongly expanded (Fig. 6F$_{2/3}$; arrowheads) while the median domains were unchanged. Overactivation of canonical Wnt signaling via *Tc-axin* RNAi led to a strong reduction of *Tc-foxQ2* (Fig. 6G$_{1,2}$) and *Tc-six3* expression (Fig.6H$_{1,2}$). In summary, we found the activation of *Tc-foxQ2* by *Tc-six3* known from other model systems and repression by Wnt signaling. In contrast to other clades *Tc-foxQ2* was required for early *Tc-six3* expression.

Tc-foxQ2 acts upstream in anterior AMR patterning

The AMR of the insect head harbors the labrum and the stomodeum. *Tc-cnc* and *Tc-croc* are upstream factors required for anterior and posterior AMR patterning, respectively (Economou and Telford, 2009; Hunnekuhl and Akam, 2014; Kittelmann et al., 2013). The AMR expression domain of *Tc-cnc* in the labrum was strongly reduced after the knockdown of *Tc-foxQ2* (Fig. 7B$_{1-4}$). Likewise, *Tc-croc* expression was affected but the reduction was restricted to the anterior boundary of expression (empty arrowheads in Fig. 7D$_{1-4}$). Its posterior expression around the stomodeum was largely unchanged. Conversely, in *Tc-croc* and *Tc-cnc* RNAi we observed no alteration of *Tc-foxQ2* expression at early stages (not shown) indicating an upstream role of *Tc-foxQ2*. However, at later stages, expression of *Tc-foxQ2* was reduced in the labrum in both treatments (Fig. S8). Next, we tested the median AMR markers *Tc-scro/nk2.1* and *Tc-fkh*. *Tc-scro/nk2.1* was reduced anteriorly and laterally in *Tc-foxQ2*^{RNAi} embryos in early elongating germ bands (Fig. 7F$_1$, empty arrowhead) but its posterior aspects were only moderately changed. In contrast to WT embryos, the stomodeal/labral expression remained connected to the lateral expression in neuroectoderm (Fig. 7F$_{2-4}$; empty arrow).

Conversely, *Tc-foxQ2* was not changed in early *Tc-scro/nk2.1*^{RNAi} embryos while in later embryos, changes were observed (Fig. S8). The expression of the stomodeum marker *Tc-fkh* was not considerably altered in *Tc-foxQ2*^{RNAi} embryos (Fig. S9) while later aspects of *Tc-foxQ2* expression were altered in *Tc-fkh* RNAi probably by indirect effects (Fig. S9).

The Notch pathway ligand *Tc-ser* and the ubiquitin ligase *Tc-mind bomb1* (*Tc-mib1*) are required for Notch signaling and knockdown of both lead to a loss of the labrum (Siemanowski et al., 2015). However, we detected no difference in *Tc-ser* expression in *Tc-foxQ2*^{RNAi} (not shown). Conversely, in early and intermediate elongating *Tc-mib1*^{RNAi} embryos only the lateral aspects of *Tc-foxQ2* expression appeared mildly decreased (Fig. S10) arguing against a strong interaction with the Notch pathway. At later stages, in contrast, some lateral and labral *Tc-foxQ2* expression domains were clearly reduced in *Tc-mib1*^{RNAi} embryos. Taken together, these results demonstrated an upstream role of *Tc-foxQ2* in early anterior AMR patterning and they indicated that the later interactions of the aGRN are different from the early ones.

An upstream role of *foxQ2* in neuroectoderm patterning

The anterior neuroectoderm is marked by the expression of several highly conserved transcription factors and harbors the anlagen of the insect head placode (Posnien et al., 2011a), the pars intercerebralis and the pars lateralis (Posnien et al., 2011b) (Fig. S3). Further, it corresponds to the region where in grasshoppers several neuroblasts arise, which are required for CX development (Boyan and Reichert, 2011). *Tc-chx* expression was completely lost in early elongating *Tc-foxQ2*^{RNAi} germ bands (empty arrowhead in Fig. 8B$_1$) and highly reduced at later stages (white arrows in Fig. 8B$_{2\text{-}4}$). The *Tc-six4* domain was highly reduced in early *Tc-foxQ2*^{RNAi} embryos, showing only small spots of expression at the anterior rim (Fig. 8D$_1$; arrow). Later, the lateral expression developed normally while a median aspect of its expression was lost (Fig. 8D$_{2\text{-}4}$; arrows). *Tc-rx* expression at

early elongating germ band stages was absent after *Tc-foxQ2*^{RNAi} (Fig. 8F$_1$). This was unexpected because *Tc-rx* is largely expressed outside the *Tc-foxQ2* expression domain (Fig. S4A$_{1-3}$) arguing against a direct effect. Indeed, our misexpression studies indicate a repressive role (see below). At later stages, the lateral aspects of *Tc-rx* expression recovered but the labral expression domain remained reduced or lost, in line with labral co-expression (Fig. 8F$_{2-3}$; empty arrowheads).

Next, we scored *Tc-foxQ2* expression in *Tc-chx*^{RNAi}, *Tc-six4*^{RNAi}, and *Tc-rx*^{RNAi} embryos. In neither treatment the early aspects of *Tc-foxQ2* expression were affected while at later stages, we found expression differences within the neurogenic region (Fig. S11). These results confirm the upstream role of *Tc-foxQ2* in early anterior patterning and they confirm that the interactions of the aGRN at later stages differ from the early ones. We found no change of cell death in the neurogenic region of *Tc-foxQ2*^{RNAi} embryos until retraction, where cell death was significantly increased 1.5 fold (p=0.023) (Fig. S12). Hence, the observed changes in expression domains are likely due to regulatory interactions but not due to loss of tissue.

Tc-foxQ2 gain-of-function analysis confirms function in anterior median neuroectoderm

Heat shock-mediated misexpression has been established in *Tribolium* (Schinko et al., 2012). We generated eight independent transgenic lines and selected one for our experiments, which showed the most evenly distributed misexpression upon heat shock (Fig. S13). Heat shock misexpression led to a reproducible pleiotropic cuticle phenotype. With respect to the anterior head the bristle pattern showed diverse signs of mild disruption (Fig. S14). Outside its expression domain, *Tc-foxQ2* misexpression led to a reduced number of segments in the legs, the abdomen and the terminus. For our experiments, we used the earliest possible time point of misexpression (9-13 h AEL), which led to a higher portion of anterior defects compared to 14-20 h AEL and 20-25 h AEL (not shown). At

14-18 h AEL (5 h after a 10 minute heat shock) the embryos were fixed and marker gene expression was scored. WT embryos undergoing the same procedure were used as negative control.

Heat shock-induced expression starts at late blastoderm stages (Schinko et al., 2012). Therefore, we were not able to test for the early interactions of the aGRN. Hence, comparably mild alterations of expression were found for *Tc-wg*, *Tc-six3* and *Tc-croc* after ectopic *Tc-foxQ2* expression (Fig. S15).

Strongest effects were found with respect to genes with late onset of expression, i.e. *Tc-rx*, *Tc-six4*, *Tc-scro*/nk2.1 and *Tc-cnc* (Fig. 9). The *Tc-rx* expression was reduced to a spotty pattern (Fig. 9A-C). This repressive function of *Tc-foxQ2* on *Tc-rx* is in line with the non-overlapping adjacent expression of these two genes (Fig. S4A_{1-3}). Therefore, we assume that the reduction of *Tc-rx* found in RNAi is due to secondary effects although this remains interpretation (see above). Ectopic *Tc-foxQ2* expression caused a premature onset and an expansion of *Tc-six4* expression (Fig. 9E,F) and an additional ectopic domain was found in the posterior head (black arrowhead in Fig. 9E,F). *Tc-scro*/*nk2.1* expression emerged precociously and was expanded in size (Fig. 9H,I). Later, the domain was altered in shape and had a spotted appearance. In case of *Tc-cnc*, a posterior expansion of the expression was observed (Fig. 9N,O; empty arrowhead).

Discussion

Dynamic *six3*/*foxQ2* interactions govern anterior development

With this work we present the first functional analysis of *Tc-foxQ2* in protostomes and together with previous work we present the most comprehensive aGRN in that clade (Fig. 10). We found that *Tc-foxQ2* is required at the top of the gene regulatory network to pattern the anterior-most part of the beetle embryo.

Interestingly, we identified a positive regulatory loop between *Tc-six3* and *Tc-foxQ2* at early embryonic stages (germ rudiment) forming a novel regulatory module. In support of this, several genetic interactions with downstream genes are similar (Posnien et al., 2011b) (see Fig. 10). The *six3/foxQ2* regulatory module regulates a large number of genes that are required for anterior AMR patterning (e.g. anterior *Tc-cnc* and *Tc-croc* expression) and neuroectoderm patterning (e.g. *Tc-chx*). Hence, it lies at the top of the aGRN governing insect anterior head and brain development and both components elicit similar phenotypes when knocked down. Such a self-regulatory module at the top of a gene network is not without precedence: For instance, *eyes absent*, *eyeless*, *dachshund,* and *sine oculis* form a positive regulatory loop at the top of the *Drosophila* eye gene regulatory network and as consequence all four genes are required for eye development leading to similar mutant phenotypes (i.e. complete loss of the eyes) (Wagner, 2007). With our data, we are not able to distinguish between alternative modes of interactions: *Tc-foxQ2* and *Tc-six3* could cooperate in the regulation of the same targets, they could individually regulate different subsets, or one gene could be the regulator of all target genes while the other would just be required for initiation of expression.

Within the regulatory module, *Tc-six3* appears to be primus inter pares based on a number of criteria: Its expression starts a bit earlier than *Tc-foxQ2* (at the differentiated blastoderm stage compared to the germ rudiment expression of *Tc-foxQ2*) and has a larger expression domain, in which early *Tc-foxQ2* is completely nested. Further, the loss of *Tc-foxQ2* in *Tc-six3* RNAi is more complete even at later stages compared to the converse experiment (Fig. 6). Finally, the *Tc-six3* cuticle phenotype is more penetrant and comprises a slightly larger region of the dorsal head (compare with Posnien et al. 2011b).

Interestingly, the mutual activation of the *six3/foxQ2* module does not persist as the initially overlapping expression patterns diverge to become largely non-overlapping at later embryonic stages (Fig. $5B_{3-7}$). Just small domains in the neuroectoderm and the labrum continue to co-express both genes (encircled in Fig. $5B_{4-7}$). Given the almost mutually exclusive expression they might even switch to mutual repression at these later stages. In line with this scenario the heat shock misexpression of *Tc-foxQ2* led to a reduction of lateral aspects of *Tc-six3* expression (Fig. S15). Hence, it could be that later repression of *six3* by *foxQ2* is conserved between sea urchin and beetles.

Protostome *foxQ2* evolved novel functions in head and brain development

Functional studies of *foxQ2* orthologs were restricted to a sea urchin as model for deuterostomes and the sea anemone, a cnidarian, representing the sister group to the bilaterian animals. This functional study in protostomes allows drawing first conclusions on the evolution of *foxQ2* function. Compared to sea urchin and sea anemone, *Tc-foxQ2* plays a much more important role in the aGRN of our protostome model. First, it is clearly required for epidermal development documented in the loss of the entire labrum in knockdown animals. This is in contrast to sea urchin and sea anemone where no epidermal phenotype was described apart from a thickened animal plate (Sinigaglia et al., 2013; Yaguchi et al., 2008). Second, *Tc-foxQ2* is required for the development of two brain parts involved in higher order processing, namely the CX and the MBs. In other models, *FoxQ2* affects specification of certain neural cell types but does not lead to tissue loss. (Sinigaglia et al., 2013; Yaguchi et al., 2008; Yaguchi et al., 2010). Finally, *Tc-foxQ2* is required for *Tc-six3* expression in *Tribolium*, which is not the case in the other models (Range and Wei, 2016; Sinigaglia et al., 2013; Yaguchi et al., 2008). Much of these novel functions may be explained by *Tc-foxQ2* gaining control over *Tc-six3* expression in our protostome model system.

The evolutionary scenario: *foxQ2* gaining functions in animal evolution

Based on previous expression data, it has been suggested that *foxQ2* orthologs played a role in anterior development in all animals and that this involved interaction with *six3* orthologs (Fig. S16) (Fritzenwanker et al., 2014; Hunnekuhl and Akam, 2014; Marlow et al., 2014; Martín-Durán et al., 2015; Santagata et al., 2012; Sinigaglia et al., 2013; Tu et al., 2006; Wei et al., 2009). In line with a conserved function, at early stages, *foxQ2* shows co-expression with *six3* in deuterostomes and cnidarians and a nested expression within protostomes. In all cases, *foxQ2* arises within the *six3* domain (Fig. S16 left column). At later stages, in contrast, expression is more diverse. Some species retain nested or co-expression with *six3* (Sinigaglia et al., 2013; Marlow et al., 2014; Martin-Duran et al., 2015) while other species develop *six3* negative/*foxQ2* positive domains (Hunnekuhl and Akam, 2014; Martin-Duran et al., 2015; Fritzenwanker et al., 2014; Wei et al., 2009; Yaguchi et al., 2008) similar to what we found in the beetle. In other species, the anterior-most region is cleared from expression of both genes (Fig. S16 right column). This variation is not clearly linked to certain clades indicating that the regulatory interactions at later stages may have evolved independently. In addition to the novel functions described above, there are conserved functional aspects as well: Initial activation of *foxQ2* by *six3* is found in all three functional model species. Repression of *six3* by *foxQ2* was found in *Strongylocentrotus* and *Tribolium* (at later stages) but not *Nematostella* (Range and Wei, 2016; Sinigaglia et al., 2013).

Together, these data indicate that at the base of metazoans *foxQ2* and *six3* were involved in early anterior patterning with *six3* being upstream of *foxQ2*. In bilaterians, the expression of both genes may have become restricted to the anterior by repression by posterior Wnt signaling (Leclère et al., 2016; Darras et al., 2011; Fritzenwanker et al., 2014; Marlow et al., 2014; Range and Wei, 2016; Sinigaglia et al., 2013; Wei et al., 2009; Yaguchi et al., 2008). After the split from Cnidaria, the Urbilateria *foxQ2* evolved a repressive function on *six3* leading to more complex expression and increased diversity of the molecular code specifying cells at the anterior pole (Range and Wei, 2016).

This diversification may have been required for the evolution of more diverse neural cell types. In protostomes, *foxQ2* additionally evolved control over early *six3* expression. Indeed, the role of *six3* as primus inter pares in the regulatory module of *Tribolium* may be a remnant of the ancestrally more important role of *six3*. A curiosity is the loss of such a highly conserved gene in the genome of placental mammalians while other vertebrates still have the gene (Mazet et al., 2003; Yu et al., 2008). Unfortunately, *foxQ2* function in vertebrates remains unstudied and our evolutionary hypothesis needs to be tested in other models representing deuterostomes, Lophotrochozoa and Ecdysozoa.

Materials and Methods

Animals and ethical statement

All the presented work is based on animals of the insect species *Tribolium castaneum*. Hence, an ethical approval was not required.

Animals were reared under standard conditions at 32°C (Brown et al., 2009). The *San Bernadino* (*SB*) wild-type strain was used for all experiments except for initial reproduction of the phenotype, where the *black* (Sokoloff, 1974) and the *Pig-19/pBA19* (Lorenzen et al., 2003) strains were used like in the iBeetle screen. The Tc-*vermillion*^{white} (v_w) strain (Lorenzen et al., 2002) was used for transgenesis and heat shock experiments. Transgenic lines marking parts of the brain (*MB-green* line (G11410); *brainy* line) were described in (Koniszewski et al., 2016).

Sequence and phylogenetic analysis

Tc-foxQ2 full coding sequence (1633 bp; Gen bank accession number: XM_008202469) was obtained from the *Tribolium* genome browser (http://bioinf.uni-greifswald.de/gb2/gbrowse/tcas5/) and the sequence was confirmed by cloning the full coding sequence from cDNA. Phylogenetic analysis was done by using MEGA v.5 (Tamura et al., 2011). The multiple sequence alignment was conducted with the ClustalW algorithm with the preset parameters. Positions containing gaps were eliminated from the dataset. The phylogenetic tree was constructed using the Neighbor-Joining method with the Dayhoff matrix based substitution model (Schwartz and Dayhoff, 1979). Bootstrap tests (Felsenstein, 1985) were conducted using 1000 replicates to test the robustness of the phylogenetic tree. *Tc-Lin31* was the second best hit in the NCBI BLASTp (Altschul et al., 1997) search (http://blast.ncbi.nlm.nih.gov/Blast.cgi) and used as outgroup.

RNAi

To test for RNAi efficiency, we detected *Tc-foxQ2* mRNA in *Tc-foxQ2* RNAi embryos (6-26 h AEL). As expected, no signal was detected using regular detection settings (not shown) but increased exposure time revealed residual *Tc-foxQ2* expression at advanced embryonic stages (Fig. S5; note the increased background in B,D,F,H). These domains reflected only part of the WT expression pattern indicating autoregulatory interactions restricted to some domains. Our subsequent analyses focused on early patterning where the RNAi knockdown was shown to be very efficient (Fig. S5A,B). Furthermore, RT-qPCR experiments confirmed efficient knockdown of the *Tc-foxQ2* mRNA level (-91.3%) using the *Tc-foxQ2*$^{RNAi\_a}$ dsRNA fragment (Fig. S6). Embryonic RNAi phenotypes were found with a penetrance of >90%, except for *Tc-foxQ2*, *Tc-rx*, and *Tc-six4*, which showed a penetrance of >40%.

The templates for the non-overlapping dsRNA fragments, used in this study, were generated by PCR from a plasmid template (For primer and dsRNA template sequences see Table S8.) The dsRNAs were synthesized using the MEGAscript® T7 Transcription Kit (Invitrogen™, Schwerte, Germany) or purchased from Eupheria BioTech (Dresden, Germany). The transcribed dsRNA was extracted via isopropanol precipitation (*Tc-foxQ2*$^{RNAi\_a}$) or phenol/chloroform extraction (*Tc-foxQ2*$^{RNAi\_b}$) and dissolved in injection buffer (1.4 mM NaCl, 0.07 mM Na_2HPO_4, 0.03 mM KH_2PO_4, 4 mM KCl, pH 6.8). The injected dsRNA concentrations for parental RNAi with *Tc-foxQ2*$^{RNAi\_a}$ and *Tc-foxQ2*$^{RNAi\_b}$ were 1.0 µg/µl, 1.5 µg/µl and 3.1 µg/µl. If not stated differently, a dsRNA concentration of 1.5 µg/µl was used. Pupal injections were performed as previously described (Bucher et al., 2002; Posnien et al., 2009b). The dsRNA was injected using FemtoJet® express (eppendorf, Hamburg, Germany). Cuticles of the L1 larval offspring were prepared as described (Wohlfrom et al., 2006).

Staining

Standard immunostaining was performed using the cleaved *Drosophila* Dcp-1 (Asp216) rabbit antibody (Cell Signaling Technology, Danvers, MA, USA; #9578) with 1:100 dilution. Anti-rabbit coupled with Alexa Fluor 488 was used for detection with 1:1000 dilution. ISH (alkaline phosphatase/NBT/BCIP) and double ISH (alkaline phosphatase/NBT/BCIP & horseradish peroxidase mediated tyramide signal amplification (TSA) reaction) (Dylight550 conjugate synthesized by Georg Oberhofer) were performed as described previously (Oberhofer et al., 2014; Schinko et al., 2009; Siemanowski et al., 2015).

Quantification of apoptosis

The regions of interest were set based on head morphology. Cell counting was performed using the Fiji cell counter plug-in (Schindelin et al., 2012). The number of apoptotic cells was positively correlated with age. Hence, to circumvent systematic errors due to staging the apoptotic cell number in the posterior procephalon was used to normalize the data. This region was chosen,

because it was outside the *foxQ2* expression domain and unaffected by our RNAi experiments. The correction value was calculated by dividing the mean number of apoptotic cells of RNAi embryos by the mean number of apoptotic cells in WT embryos in the control region. For the normalization, the data was divided by the correction value. Raw counts are shown in Table S7.

The normalized data was tested with R (v.2.14.2; http://www.R-project.org/) for the homogeneity of the variances via the box plot, and for normal distribution, via the Shapiro-Wilk test. To test for significance, three statistical tests were conducted: Welch t-test, two sample t-test and the Wilcoxon rank-sum test. All three tests showed the same levels of significance. Stated *p*-values are based on the Wilcoxon rank-sum test results.

Transgenesis and heat shock

The *foxQ2* heat shock construct was based on the constructs developed by Schinko et al., 2012 and germline transformation was performed as described previously (Berghammer et al., 1999; Schinko et al., 2012) using the injection buffer used for RNAi experiments and the mammalian codon-optimized hyperactive transposase (Yusa et al., 2011) flanked by the *Tc-hsp68* sequences (gift from Stefan Dippel). All animals for heat shock experiments were kept at 32°C. Heat shock was performed as described previously (Schinko et al., 2012) for ten minutes at 48°C (egg collections for cuticle preparations: 0-24 h AEL, 9-13 h AEL, 14-20 h AEL, 20-25 h AEL; egg collections for ISHs: 9-13 h AEL (fixated 5 h after heat shock)). For each gene, one batch of embryos was used. In the figure we show alterations that represent >50% of the phenotypes found in the batch.

Image documentation and processing

Cuticle preparations and L1 larval brains were imaged as described (Posnien et al., 2011b; Wohlfrom et al., 2006) using the LSM510 or Axioplan 2 (ZEISS, Jena, Germany) and processed using Amira (v.5.3.2; FEI) using 'voltex' projections. Stacks were visualized as average or maximum projections

using Fiji (v. 1.49i; (Schindelin et al., 2012)). All images were level-adjusted and assembled in Photoshop CS (Adobe) and labelled using Illustrator CS5 (Adobe).

List of Symbols and Abbreviatons

AEL - after egg laying

aGRN - anterior gene regulatory network

AMR - anterior median region

arr - arrow

CB - central body

cnc - cap'n'collar

col - collier

croc - crocodile

CX - central complex

Dcp1 - cleaved *Drosophila* death caspase-1

fkh - forkhead

foxa - forkhead box a

foxq2 - forkhead box q2

MB - mushroom body

mib1 - mindbomb 1

nk2.1 - nk2 homeobox 1 (thyroid transcription factor1

rx - retinal homeobox

scro - scarecrow

ser - serrate

six3 - sine oculis homeobox homolog 3

six4 - sine oculis homeobox homolog 4

tll - tailless

TSA - tyramide signal amplification

wg - wingless

wnt1 - int1 (wingless-related1)

Acknowledgements

We thank Claudia Hinners for excellent technical help and Stefan Dippel for the hyperactive helper construct. The phenotype was initially identified in the iBeetle project (DFG research unit FOR1234) and the work was supported by DFG grants BU1443/11, BU1443/8 and the Göttingen Graduate School for Neurosciences, Biophysics, and Molecular Biosciences (GGNB).

References

Altschul, S. F., Madden, T. L., Schaffer, A. A., Zhang, J., Zhang, Z., Miller, W. and Lipman, D. J. (1997). Gapped BLAST and PSI-BLAST: a new generation of protein database search programs. Nucleic Acids Res **25**, 3389–402.

Benayoun, B. A., Caburet, S. and Veitia, R. A. (2011). Forkhead transcription factors: key players in health and disease. *Trends Genet.* **27**, 224–232.

Berghammer, A. J., Klingler, M. and Wimmer, E. A. (1999). A universal marker for transgenic insects. *Nature* **402**, 370–371.

Bolognesi, R., Fischer, T. D. and Brown, S. J. (2009). Loss of Tc-arrow and canonical Wnt signaling alters posterior morphology and pair-rule gene expression in the short-germ insect, Tribolium castaneum. *Dev Genes Evol* **219**, 369–75.

Boyan, G. S. and Reichert, H. (2011). Mechanisms for complexity in the brain: generating the insect central complex. *Trends Neurosci.* **34**, 247–257.

Brown, S., Fellers, J., Shippy, T., Denell, R., Stauber, M. and Schmidt-Ott, U. (2001). A strategy for mapping bicoid on the phylogenetic tree. *Curr Biol* **11**, R43-4.

Brown, S. J., Shippy, T. D., Miller, S., Bolognesi, R., Beeman, R. W., Lorenzen, M. D., Bucher, G., Wimmer, E. A. and Klingler, M. (2009). The Red Flour Beetle, Tribolium castaneum (Coleoptera): A Model for Studies of Development and Pest Biology. *Cold Spring Harb. Protoc.* **2009**, pdb.emo126-emo126.

Bucher, G., Scholten, J. and Klingler, M. (2002). Parental RNAi in Tribolium (Coleoptera). *Curr. Biol.* **12**, R85–R86.

Coulcher, J. F. and Telford, M. J. (2012). Cap'n'collar differentiates the mandible from the maxilla in the beetle Tribolium castaneum. *Evodevo* **3**, 25.

Darras, S., Gerhart, J., Terasaki, M., Kirschner, M. and Lowe, C. J. (2011). -Catenin specifies the endomesoderm and defines the posterior organizer of the hemichordate Saccoglossus kowalevskii. *Development* **138**, 959–970.

Dönitz, J., Schmitt-Engel, C., Grossmann, D., Gerischer, L., Tech, M., Schoppmeier, M., Klingler, M. and Bucher, G. (2015). iBeetle-Base: a database for RNAi phenotypes in the red flour beetle Tribolium castaneum. *Nucleic Acids Res.* **43**, D720–D725.

Economou, A. D. and Telford, M. J. (2009). Comparative gene expression in the heads of Drosophila melanogaster and Tribolium castaneum and the segmental affinity of the Drosophila hypopharyngeal lobes. *Evol Dev* **11**, 88–96.

Felsenstein, J. (1985). Confidence Limits on Phylogenies: An Approach Using the Bootstrap. *Evolution* **39**, 783.

Florentin, A. and Arama, E. (2012). Caspase levels and execution efficiencies determine the apoptotic potential of the cell. *J. Cell Biol.* **196**, 513–527.

Fritzenwanker, J. H., Gerhart, J., Freeman, R. M. and Lowe, C. J. (2014). The Fox/Forkhead transcription factor family of the hemichordate Saccoglossus kowalevskii. *EvoDevo* **5**, 17.

Fu, J., Posnien, N., Bolognesi, R., Fischer, T. D., Rayl, P., Oberhofer, G., Kitzmann, P., Brown, S. J. and Bucher, G. (2012). Asymmetrically expressed axin required for anterior development in Tribolium. *Proc. Natl. Acad. Sci. U. S. A.* **109**, 7782–7786.

Heisenberg, M. (2003). Mushroom body memoir: from maps to models. *Nat. Rev. Neurosci.* **4**, 266–275.

Hunnekuhl, V. S. and Akam, M. (2014). An anterior medial cell population with an apical-organ-like transcriptional profile that pioneers the central nervous system in the centipede Strigamia maritima. *Dev. Biol.* **396**, 136–149.

Kittelmann, S., Ulrich, J., Posnien, N. and Bucher, G. (2013). Changes in anterior head patterning underlie the evolution of long germ embryogenesis. *Dev. Biol.* **374**, 174–184.

Kitzmann, P., Schwirz, J., Schmitt-Engel, C. and Bucher, G. (2013). RNAi phenotypes are influenced by the genetic background of the injected strain. *BMC Genomics* **14**, 5.

Koniszewski, N. D. B., Kollmann, M., Bigham, M., Farnworth, M., He, B., Büscher, M., Hütteroth, W., Binzer, M., Schachtner, J. and Bucher, G. (2016). The insect central complex as model for heterochronic brain development—background, concepts, and tools. *Dev. Genes Evol.*

Leclère, L., Bause, M., Sinigaglia, C., Steger, J. and Rentzsch, F. (2016). Development of the aboral domain in Nematostella requires β-catenin and the opposing activities of Six3/6 and Frizzled5/8. Dev. Camb. Engl. **143**, 1766–1777.

Lee, H.-H. and Frasch, M. (2004). Survey of forkhead domain encoding genes in theDrosophila genome: Classification and embryonic expression patterns. *Dev. Dyn.* **229**, 357–366.

Lorenzen, M. D., Brown, S. J., Denell, R. E. and Beeman, R. W. (2002). Cloning and characterization of the Tribolium castaneum eye-color genes encoding tryptophan oxygenase and kynurenine 3-monooxygenase. *Genetics* **160**, 225–234.

Lorenzen, M. D., Berghammer, A. J., Brown, S. J., Denell, R. E., Klingler, M. and Beeman, R. W. (2003). piggyBac-mediated germline transformation in the beetle Tribolium castaneum. *Insect Mol. Biol.* **12**, 433–440.

Lowe, C. J., Wu, M., Salic, A., Evans, L., Lander, E., Stange-Thomann, N., Gruber, C. E., Gerhart, J. and Kirschner, M. (2003). Anteroposterior patterning in hemichordates and the origins of the chordate nervous system. *Cell* **113**, 853–65.

Marlow, H., Matus, D. Q. and Martindale, M. Q. (2013). Ectopic activation of the canonical wnt signaling pathway affects ectodermal patterning along the primary axis during larval development in the anthozoan Nematostella vectensis. *Dev. Biol.* **380**, 324–334.

Marlow, H., Tosches, M. A., Tomer, R., Steinmetz, P. R., Lauri, A., Larsson, T. and Arendt, D. (2014). Larval body patterning and apical organs are conserved in animal evolution. *BMC Biol.* **12**, 7.

Martin, B. L. and Kimelman, D. (2009). Wnt signaling and the evolution of embryonic posterior development. *Curr Biol* **19**, R215-9.

Martín-Durán, J. M., Vellutini, B. C. and Hejnol, A. (2015). Evolution and development of the adelphophagic, intracapsular Schmidt's larva of the nemertean Lineus ruber. *EvoDevo* **6**,.

Mazet, F., Yu, J.-K., Liberles, D. A., Holland, L. Z. and Shimeld, S. M. (2003). Phylogenetic relationships of the Fox (Forkhead) gene family in the Bilateria. *Gene* **316**, 79–89.

Momose, T., Derelle, R. and Houliston, E. (2008). A maternally localised Wnt ligand required for axial patterning in the cnidarian Clytia hemisphaerica. *Development* **135**, 2105–2113.

Oberhofer, G., Grossmann, D., Siemanowski, J. L., Beissbarth, T. and Bucher, G. (2014). Wnt/ -catenin signaling integrates patterning and metabolism of the insect growth zone. *Development* **141**, 4740–4750.

Petersen, C. P. and Reddien, P. W. (2009). Wnt signaling and the polarity of the primary body axis. *Cell* **139**, 1056–1068.

Pfeiffer, K. and Homberg, U. (2014). Organization and Functional Roles of the Central Complex in the Insect Brain. *Annu. Rev. Entomol.* **59**, 165–184.

Posnien, N., Bashasab, F. and Bucher, G. (2009a). The insect upper lip (labrum) is a nonsegmental appendage-like structure. *Evol Dev* **11**, 479–487.

Posnien, N., Schinko, J., Grossmann, D., Shippy, T. D., Konopova, B. and Bucher, G. (2009b). RNAi in the Red Flour Beetle (Tribolium). *Cold Spring Harb. Protoc.* **2009**, pdb.prot5256-prot5256.

Posnien, N., Schinko, J. B., Kittelmann, S. and Bucher, G. (2010). Genetics, development and composition of the insect head - A beetle's view. *Arthropod Struct Dev* **39**, 399–410.

Posnien, N., Koniszewski, N. and Bucher, G. (2011a). Insect Tc-six4 marks a unit with similarity to vertebrate placodes. *Dev Biol* **350**, 208–216.

Posnien, N., Koniszewski, N. D. B., Hein, H. J. and Bucher, G. (2011b). Candidate Gene Screen in the Red Flour Beetle Tribolium Reveals Six3 as Ancient Regulator of Anterior Median Head and Central Complex Development. *PLoS Genet.* **7**, e1002418.

Range, R. C. and Wei, Z. (2016). An anterior signaling center patterns and sizes the anterior neuroectoderm of the sea urchin embryo. *Development*.

Santagata, S., Resh, C., Hejnol, A., Martindale, M. Q. and Passamaneck, Y. J. (2012). Development of the larval anterior neurogenic domains of Terebratalia transversa (Brachiopoda) provides insights into the diversification of larval apical organs and the spiralian nervous system. *EvoDevo* **3**, 3.

Schaeper, N. D., Pechmann, M., Damen, W. G., Prpic, N. M. and Wimmer, E. A. (2010). Evolutionary plasticity of collier function in head development of diverse arthropods. *Dev Biol* **344**, 363–76.

Schindelin, J., Arganda-Carreras, I., Frise, E., Kaynig, V., Longair, M., Pietzsch, T., Preibisch, S., Rueden, C., Saalfeld, S., Schmid, B., et al. (2012). Fiji: an open-source platform for biological-image analysis. *Nat. Methods* **9**, 676–682.

Schinko, J., Posnien, N., Kittelmann, S., Koniszewski, N. and Bucher, G. (2009). Single and Double Whole-Mount In Situ Hybridization in Red Flour Beetle (Tribolium) Embryos. *Cold Spring Harb. Protoc.* **2009**, pdb.prot5258-prot5258.

Schinko, J. B., Hillebrand, K. and Bucher, G. (2012). Heat shock-mediated misexpression of genes in the beetle Tribolium castaneum. *Dev. Genes Evol.* **222**, 287–298.

Schmitt-Engel, C., Schultheis, D., Schwirz, J., Ströhlein, N., Troelenberg, N., Majumdar, U., Dao, V. A., Grossmann, D., Richter, T., Tech, M., et al. (2015). The iBeetle large-scale RNAi screen reveals gene functions for insect development and physiology. *Nat. Commun.* **6**, 7822.

Schoppmeier, M. and Schröder, R. (2005). Maternal torso signaling controls body axis elongation in a short germ insect. *Curr Biol* **15**, 2131–6.

Schwartz, R. M. and Dayhoff, M. O. (1979). Protein and nucleic Acid sequence data and phylogeny. *Science* **205**, 1038–1039.

Siemanowski, J., Richter, T., Dao, V. A. and Bucher, G. (2015). Notch signaling induces cell proliferation in the labrum in a regulatory network different from the thoracic legs. *Dev. Biol.* **408**, 164–177.

Sinigaglia, C., Busengdal, H., Leclère, L., Technau, U. and Rentzsch, F. (2013). The Bilaterian Head Patterning Gene six3/6 Controls Aboral Domain Development in a Cnidarian. *PLoS Biol.* **11**, e1001488.

Sokoloff, A. (1974). *The biology of Tribolium, with special emphasis on genetic aspects.*

Stauber, M., Jackle, H. and Schmidt-Ott, U. (1999). The anterior determinant bicoid of Drosophila is a derived Hox class 3 gene. *Proc Natl Acad Sci U A* **96**, 3786–9.

Steinmetz, P. R., Urbach, R., Posnien, N., Eriksson, J., Kostyuchenko, R. P., Brena, C., Guy, K., Akam, M., Bucher, G. and Arendt, D. (2010). Six3 demarcates the anterior-most developing brain region in bilaterian animals. *EvoDevo* **1**, 14.

Tamura, K., Peterson, D., Peterson, N., Stecher, G., Nei, M. and Kumar, S. (2011). MEGA5: Molecular Evolutionary Genetics Analysis Using Maximum Likelihood, Evolutionary Distance, and Maximum Parsimony Methods. *Mol. Biol. Evol.* **28**, 2731–2739.

Telford, M. J., Bourlat, S. J., Economou, A., Papillon, D. and Rota-Stabelli, O. (2008). The evolution of the Ecdysozoa. *Philos Trans R Soc Lond B Biol Sci* **363**, 1529–37.

Tu, Q., Brown, C. T., Davidson, E. H. and Oliveri, P. (2006). Sea urchin Forkhead gene family: Phylogeny and embryonic expression. *Dev. Biol.* **300**, 49–62.

van der Zee, M., Berns, N. and Roth, S. (2005). Distinct functions of the Tribolium zerknullt genes in serosa specification and dorsal closure. Curr Biol **15**, 624–36.

Wagner, G. P. (2007). The developmental genetics of homology. *Nat. Rev. Genet.* **8**, 473–479.

Wei, Z., Yaguchi, J., Yaguchi, S., Angerer, R. C. and Angerer, L. M. (2009). The sea urchin animal pole domain is a Six3-dependent neurogenic patterning center. *Development* **136**, 1583–1583.

Wohlfrom, H., Schinko, J. B., Klingler, M. and Bucher, G. (2006). Maintenance of segment and appendage primordia by the Tribolium gene knödel. *Mech. Dev.* **123**, 430–439.

Yaguchi, S., Yaguchi, J., Angerer, R. C. and Angerer, L. M. (2008). A Wnt-FoxQ2-Nodal Pathway Links Primary and Secondary Axis Specification in Sea Urchin Embryos. *Dev. Cell* **14**, 97–107.

Yaguchi, S., Yaguchi, J., Wei, Z., Shiba, K., Angerer, L. M. and Inaba, K. (2010). ankAT-1 is a novel gene mediating the apical tuft formation in the sea urchin embryo. *Dev. Biol.* **348**, 67–75.

Yaguchi, J., Angerer, L. M., Inaba, K. and Yaguchi, S. (2012). Zinc finger homeobox is required for the differentiation of serotonergic neurons in the sea urchin embryo. *Dev. Biol.* **363**, 74–83.

Yaguchi, J., Takeda, N., Inaba, K. and Yaguchi, S. (2016). Cooperative Wnt-Nodal Signals Regulate the Patterning of Anterior Neuroectoderm. *PLoS Genet.* **12**, e1006001.

Yu, J.-K., Mazet, F., Chen, Y.-T., Huang, S.-W., Jung, K.-C. and Shimeld, S. M. (2008). The Fox genes of Branchiostoma floridae. *Dev. Genes Evol.* **218**, 629–638.

Yusa, K., Zhou, L., Li, M. A., Bradley, A. and Craig, N. L. (2011). A hyperactive piggyBac transposase for mammalian applications. *Proc. Natl. Acad. Sci.* **108**, 1531–1536.

Figures

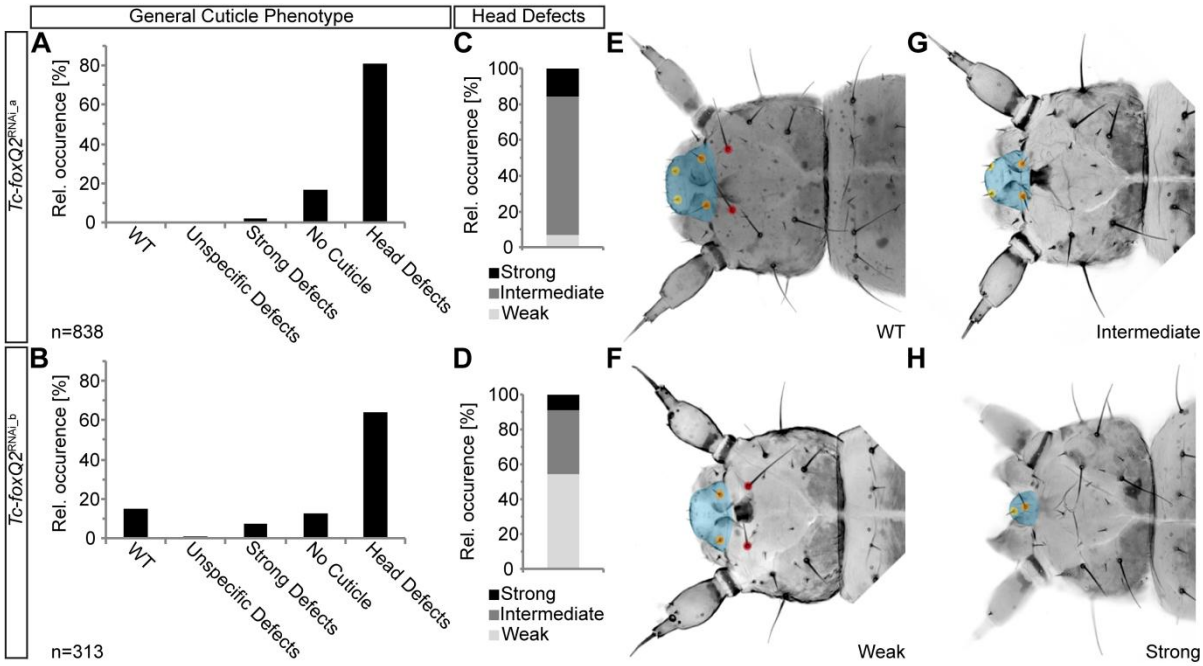

Fig. 1. *Tc-foxQ2* RNAi phenotype and off-target control. (**A**, **B**) Knockdown of *Tc-foxQ2* with two non-overlapping dsRNA fragments *Tc-foxQ2*$^{RNAi\_a}$ (**A**) *and Tc-foxQ2*$^{RNAi\_b}$ (**B**) leads to comparable portions of cuticle phenotypes. (**C**, **D**) Detailed analysis of the head defects shows that the *Tc-foxQ2*$^{RNAi\_a}$ dsRNA fragment leads to a qualitatively comparable but quantitatively stronger phenotype, marked by more intermediate and strong head defects. (**E-H**) L1 cuticle heads, depicted in a dorsal view,representing the different classes of head defects. Anterior is left. (**E**) WT cuticle with the labrum marked in blue, two labrum setae (yellow dots), two clypeus setae (orange dots) and two anterior vertex setae (red dots). (**F**) Weak head defect with a reduced labrum and at least one deleted labrum seta. (**G**) Intermediate head defect is additionally lacking at least one of the anterior vertex seta. (**H**) Strong head defect with a strongly reduced labrum, one labrum seta and

one clypeus seta left. In the strongest phenotypes the labrum and the anterior vertex setae are deleted.

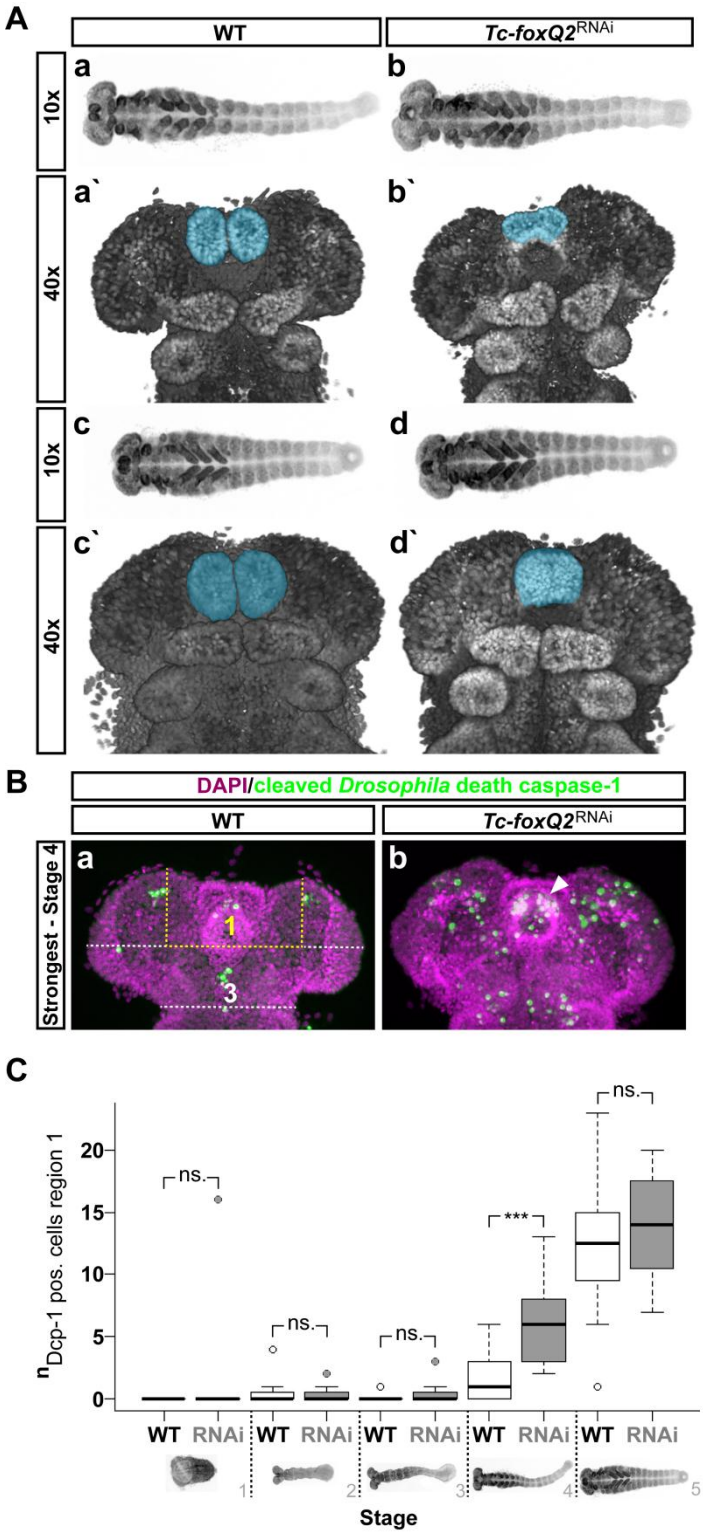

Fig. 2. Cell death in *Tc-foxQ2*^{RNAi} phenotype. (A) Morphology of WT ($A_{a/c}$) and *Tc-foxQ2*^{RNAi} ($A_{b/d}$) embryos is visualized by nuclear staining (DAPI, grey). Anterior is left in 10x and up in 40x panels. The labrum is marked in blue. *Tc-foxQ2*^{RNAi} embryos (6-26 h AEL) show decreased labral buds, which

appear to fuse prematurely ($A_{b`/d`}$) . (B) For quantification of cell death, a region of interest (region 1, yellow dashed lines) and a control region (region 3, white dashed lines) were defined. Apoptotic cells were monitored by antibody staining (cleaved death caspase-1 (Dcp-1); green). A fully elongated *Tc-foxQ2*^{RNAi} WT germ band with most apoptotic cells within the labral region (B_a; region 1) compared to the *Tc-foxQ2*^{RNAi} embryo that showed most apoptotic cells within region 1 (B_b; arrowhead). (C) Box plot depicting the normalized number of apoptotic cells at five different embryonic stages, subdivided in untreated (WT) and *Tc-foxQ2*^{RNAi} embryos (RNAi). The values are normalized with the region 3 values. Brackets display grade of significance. Germ rudiments (stage 1) to intermediate elongating germ bands (stage 3), as well as early retracting germ bands (stage 5) show no significant increase in the number of apoptotic cells (stage 1: p=0.33 (WT: n=3, RNAi: n=7), stage 2: p=0.63 (WT: n=11, RNAi: n=12), stage 3: p=0.19 (WT: n=9, RNAi: n=19), stage 5: p=0.15 (WT: n=12, RNAi: n=11)). However, fully elongated germ bands showed significantly more apoptotic cells (p=0.00041) in *Tc-foxQ2*^{RNAi} embryos (n=15) compared to untreated ones (n=17). The line inside the box represents the median, the box is defined by the first and the third quartile, the whiskers are defined by still being within 1.5 IQR of the lower/upper quartile and dots represent outliers. ns.: not significant

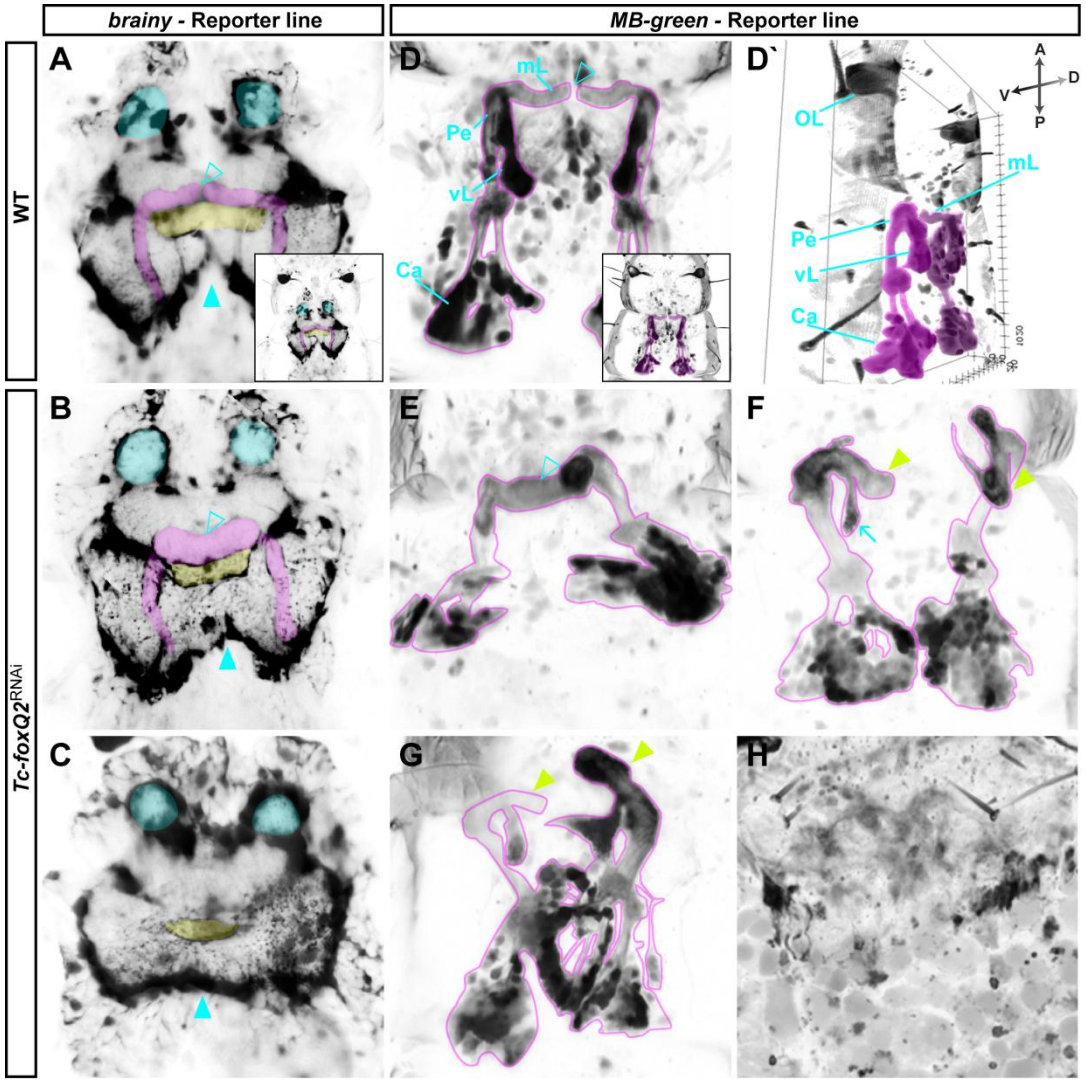

Fig. 3. Loss of *Tc-foxQ2* function leads to brain defects. Anterior is up. (**A-C**) Glial tissue (black) is visualized in L1 larvae by the transgenic *brainy* reporter line in WT (A) and *Tc-foxQ2*^{RNAi} (B,C) (A-C: Voltex projections). (**D-H**) Mushroom bodies (MBs; black) are visualized by the transgenic *MB-green* reporter line, in WT (D,D`) and *Tc-foxQ2*$^{RNAi}$ (E-H) (D-H: MAX projections, D`: 3D projection). (A) WT L1 larval brain that shows the two brain hemispheres with a MBs (magenta), antennal lobes (cyan), and the mid-line spanning central body (CB, yellow). (B) A weak *Tc-foxQ2*^{RNAi} larval brain phenotype showing the loss of the boundary between the medial lobes of the MB (compare empty arrowheads in B and A). The CB appears to be reduced in size. (C) Intermediate *Tc-foxQ2*^{RNAi} larval brains appear to lack the MBs and the CB appears to be reduced in size. (B,C) In both phenotypes the brain hemispheres appear to be fused (cyan arrowhead). (D) WT L1 larval MBs in a dorsal view. (D`) 3D

projection of WT L1 larval MBs, providing an overview of the organization of the structures. (E) A weak *Tc-foxQ2* RNAi-induced MB phenotype, where the two medial lobes appear to be fused (compare empty arrowheads in D and E). (F) MBs with distorted pedunculi, leading to a loss of contact between the two medial lobes (yellow arrowheads), and reduced vertical lobes (arrow). (G) Phenotype with interdigitating MBs. (H) In strong phenotypes the MB structures are highly reduced or absent. OL: optical lobe, mL: medial lobe, Pe: pedunculus, vL: vertical lobe, Ca: calyx

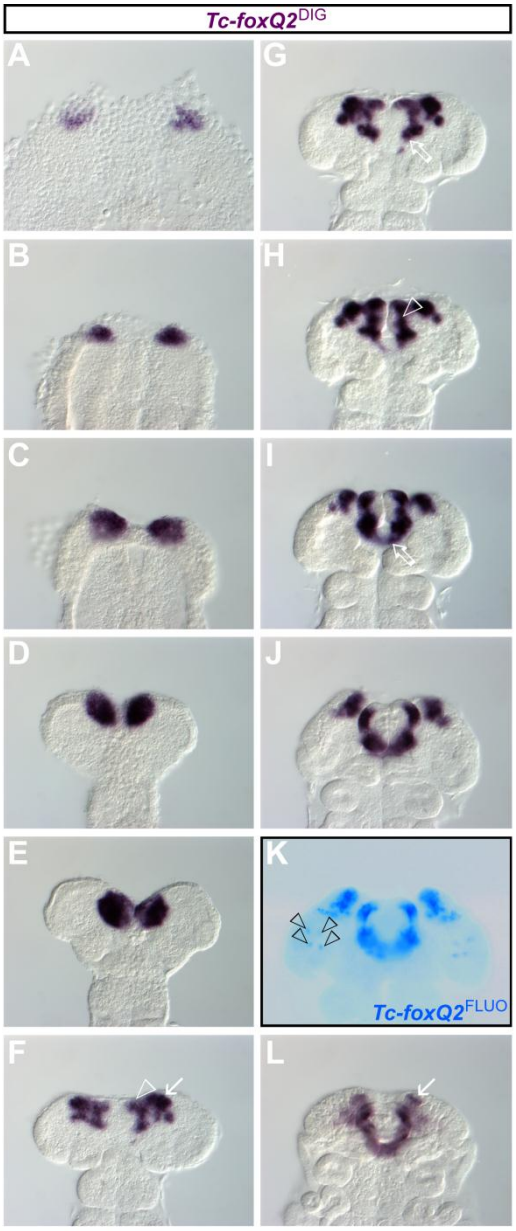

Fig. 4. *Tc-foxQ2* is expressed in a highly dynamic pattern at the anterior pole. Anterior is up. Expression of *Tc-foxQ2* in WT embryos is monitored by whole mount in situ hybridization (ISH). (**A**) *Tc-foxQ2* expression starts with the formation of the germ rudiment. (**A**-**E**) The early *Tc-foxQ2* expression starts with two domains located at the anterior pole, which successively approach each other, probably due to morphogenetic movements. (**F**) The expression splits into several domains in late elongating germ bands, with expression in the putative neuroectoderm (white arrow, presumably including parts of the pars intercerebralis; Posnien 2011) and in the labral/stomodeal region (white empty arrowhead). (**G**) The expression domains flanking the prospective stomodeum

become more prominent (empty arrow). (**H**) The anterior median expression domain frames the lateral parts of the labral buds (white empty arrowhead). (**I**, **J**) At fully elongated and early retracting germ band stages the two expression domains flanking the stomodeum become posteriorly linked (empty arrow). (**K**) The staining with the more sensitive TSA-Dylight550 reveals four dot-like expression domains in the ocular region (black empty arrowheads). (**L**) At retracting germ band stages *Tc-foxQ2* is expressed in a narrow U-shape pattern and the neuroectodermal expression domains are reduced in size (white arrow).

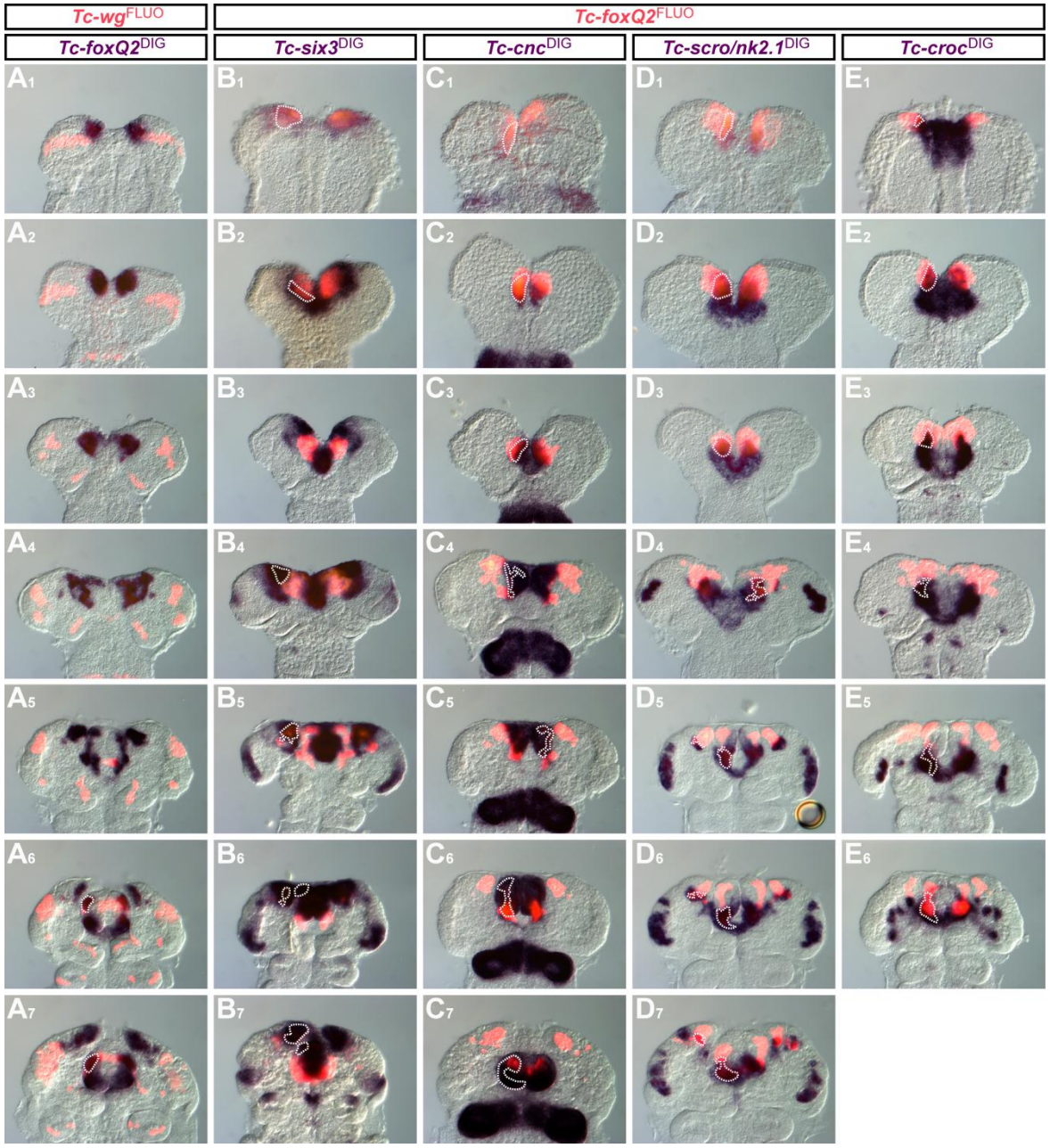

Fig. 5. Co-expression of *Tc-foxQ2* and anterior head patterning genes. Anterior is up. Expression is visualized by double ISH, using NBT/BCIP (blue) and TSA-Dylight550 (red). Co-expression is indicated with dashed lines. (**A_{1-7}**) Co-expression with *Tc-wg* is found only after full elongation (**A_{6-7}**). (**B_{1-7}**) *Tc-foxQ2* and *Tc-six3* expression completely overlaps during germ rudiment stages (**B_1**). In early elongating germ bands the co-expression is limited to a narrow lateral stripe of the anterior median region (AMR; **B_2**). Intermediate germ bands show a mutually exclusive expression of *Tc-foxQ2* and *Tc-six3* (**B_3**). At later stages, expression overlap is found within the neurogenic region (**B_{4-5}**) and later

also in the labral buds (**B**$_{6\text{-}7}$). (**C**$_{1\text{-}7}$) *Tc-cnc* expression is completely overlapping with the expression of *Tc-foxQ2* at early embryonic stages (**C**$_{1\text{-}3}$) but later co-expression is found in the labral/stomodeal region (**C**$_{4\text{-}7}$). (**D**$_{1\text{-}7}$) *Tc-scro/nk2.1* is partially co-expressed at early embryonic stages (**D**$_{1\text{-}3}$). In late elongating germ bands the co-expression is restricted to a narrow lateral stripe (**D**$_4$) and the posterior portion of the labral buds, close to the stomodeum and small areas of the neurogenic region (**D**$_{5\text{-}7}$). *Tc-croc* expression is partially overlapping with *Tc-foxQ2* at early stages (**E**$_{1\text{-}3}$) and later in a region close to the stomodeum (**E**$_{4\text{-}6}$).

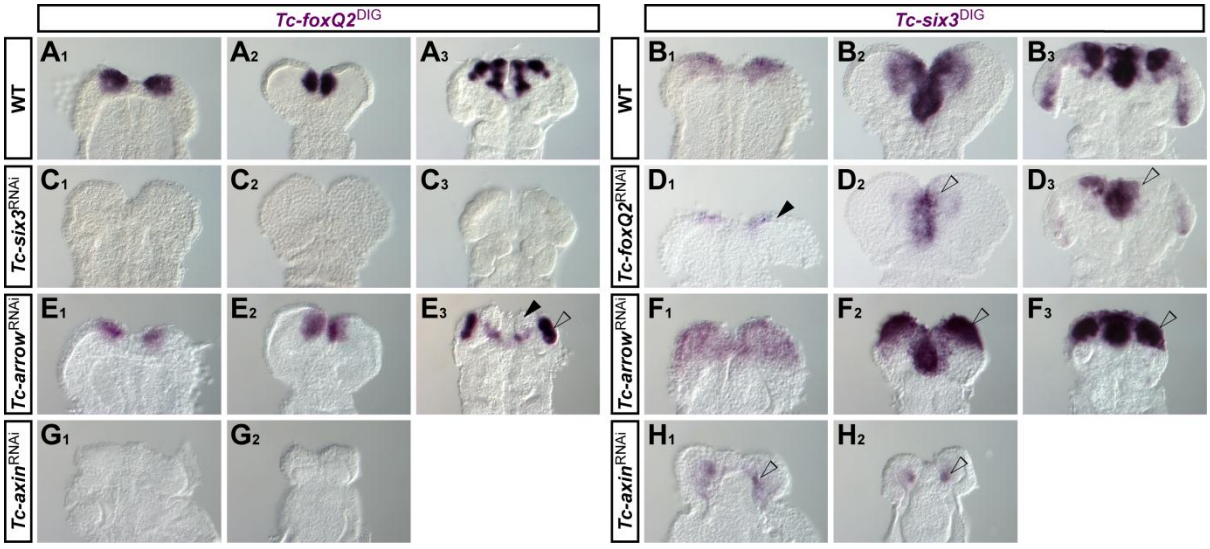

Fig 6. Mutual activation of *Tc-foxQ2* and *Tc-six3* and their repression by Wnt signaling. Anterior is up. Expression pattern of *Tc-foxQ2* in WT (**A_1-A_3**), *Tc-six3*^{RNAi} (**C_1-C_3**), *Tc-arr*^{RNAi} (**E_1-E_3**), and *Tc-axin*^{RNAi} (**G_1,G_2**) embryos and expression pattern of *Tc- six3* in WT (**B_1-B_3**), *Tc-foxQ2*^{RNAi} (**D_1-D_3**), *Tc-arr*^{RNAi} (**F_1-F_3**), and *Tc-axin*^{RNAi} (**H_1,H_2**) embryos monitored by ISH. (**$C_{1\text{-}3}$**) *Tc-foxQ2* expression was lost in *Tc-six3*^{RNAi} embryos. (**D_1**) *Tc-six3* expression was strongly reduced in *Tc-foxQ2*^{RNAi} germ rudiments (arrowhead). (**$D_{2/3}$**) Later, median expression emerged but the lateral *Tc-six3* expression remained reduced or absent (empty arrowhead) while the ocular domain appeared unchanged. (**$E_{1/2}$**) *Tc-foxQ2* expression was unchanged in early *Tc-arr*^{RNAi} embryos but the median *Tc-foxQ2* expression was reduced at later stages (**E_3**; black arrowhead) whereas the neurogenic *Tc-foxQ2* expression domain expanded (**E_3**; empty arrowhead). (**$F_{1\text{-}3}$**) In *Tc-arr*^{RNAi} embryos the *Tc-six3* expression expanded towards posterior in the neuroectoderm (empty arrowheads) while the stomodeal domain appeared to be unaffected. In *Tc-axin*^{RNAi} embryos WNT signaling is derepressed, which led to repression of *Tc-foxQ2* expression (**$G_{1/2}$**) and to a strong reduction of *Tc-six3* expression (**$H_{1/2}$**).

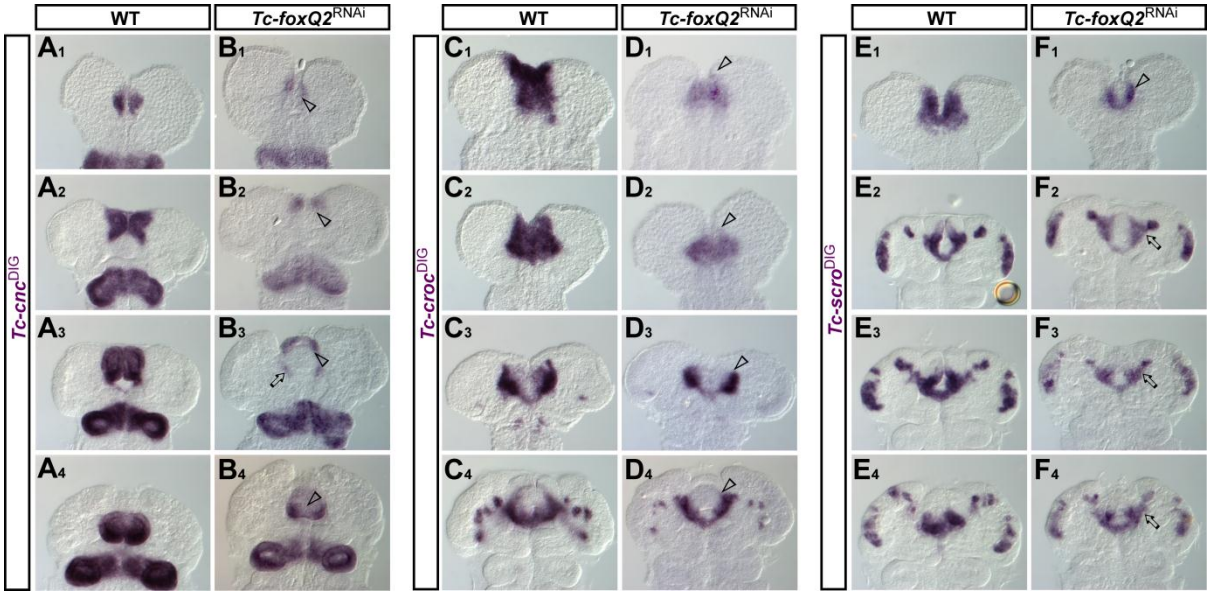

Fig. 7. *Tc-foxQ2*^{RNAi} regulates *Tc-cnc*, *Tc-croc* and *Tc-scro* expression. Anterior is up. Expression pattern of *Tc-cnc* in WT (**A$_{1-4}$**) and *Tc-foxQ2*^{RNAi} (**B$_{1-4}$**) embryos, expression of *Tc-croc* in WT (**C$_{1-4}$**) and *Tc-foxQ2*^{RNAi} (**D$_{1-4}$**) embryos, and expression of *Tc-scro* in WT (**E$_{1-4}$**) and *Tc-foxQ2*^{RNAi} (**F$_{1-4}$**) embryos monitored by ISH. (**B$_{1-2}$**) In *Tc-foxQ2*^{RNAi} embryos the anterior domain of *Tc-cnc* expression was reduced (empty arrowheads). Prior to this stage no changes in the expression pattern were observed (not shown). (**B$_{3/4}$**) In fully elongated and retracting germ bands the labral expression was strongly reduced (empty arrowheads) while stomodeal expression was slightly altered (empty arrow). (**D$_{1-4}$**) Throughout development, *Tc-croc* expression pattern was lacking the anterior portion of its AMR expression domain (empty arrowheads). (**F$_1$**) Expression of *Tc-scro*/*nk2.1* is reduced to a narrow stripe along the anterior fold (empty arrowhead). (**F$_{2-4}$**) Later stages show an atypical bridging between the labral/stomodeal and the neurogenic *Tc-scro*/*nk2.1* expression domains (empty arrows). Note that the intensity of the WT staining in J is somewhat stronger than in the other panels.

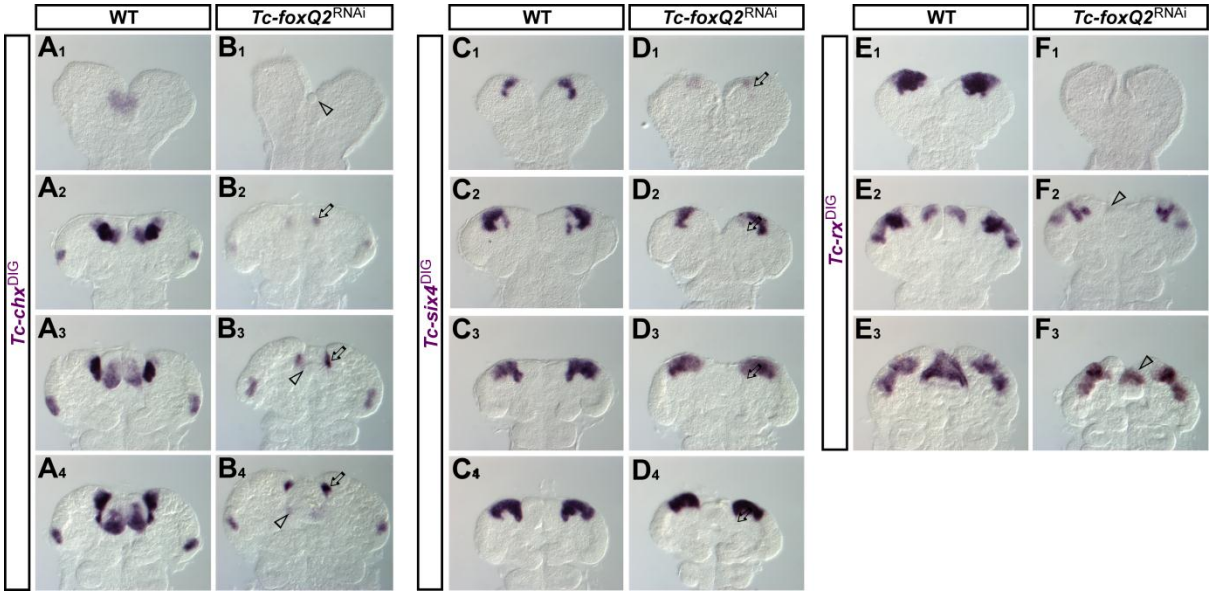

Fig. 8. *Tc-foxQ2*^{RNAi} embryos show reduced *Tc-chx*, *Tc-six4*, and *Tc-rx* expression. Anterior is up. Expression patterns of *Tc-chx* in WT (**A$_{1-4}$**) and *Tc-foxQ2*^{RNAi} embryos (**B$_{1-4}$**), of *Tc-six4* in WT (**C$_{1-4}$**) and *Tc-foxQ2*^{RNAi} embryos (**D$_{1-4}$**) and of *Tc-rx* in WT (**E$_{1-3}$**) and *Tc-foxQ2*^{RNAi} embryos (**F$_{1-3}$**) monitored by ISH. (**B$_1$**) *Tc-chx* expression was completely absent in early elongating *Tc-foxQ2*^{RNAi} germ bands (empty arrowhead). (**B$_{2-4}$**) At later stages, the labral *Tc-chx* expression domains were almost absent (empty arrowheads) while the anterior neurogenic expression domains were strongly reduced (arrows). The ocular *Tc-chx* expression domained remain unaffected. (**D$_1$**) Expression of *Tc-six4* is strongly reduced in early elongating germ bands (arrow). (**D$_{2-4}$**) At later stages, only the median posterior extensions of the *Tc-six4* expression domains were reduced (arrows). (**F$_1$**) *Tc-rx* expression is strongly reduced or completely absent in early elongating *Tc-foxQ2*^{RNAi} germ bands. (**F$_{2-3}$**) At later stages, the neurogenic *Tc-rx* expression pattern appeared unaffected, but the labral expression domains were absent (**F$_2$**: empty arrowhead) or reduced in size (**F$_3$**: empty arrowhead).

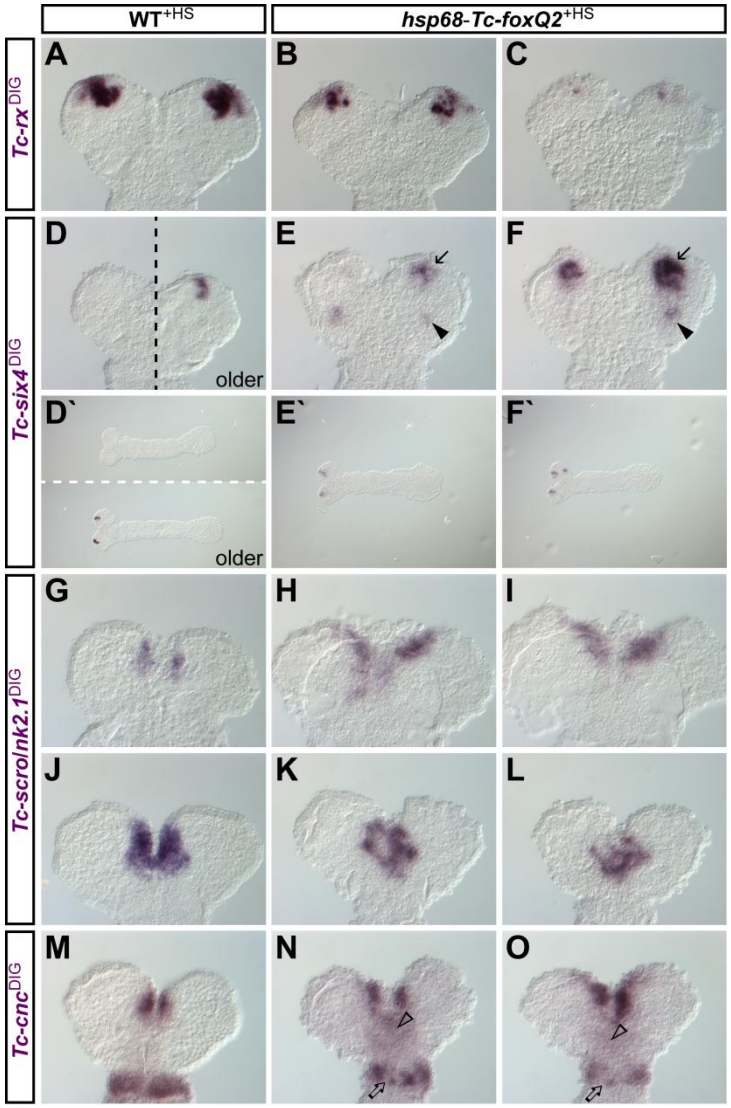

Fig. 9. Ectopic *Tc-foxQ2* expression impacts head patterning. Anterior is up in all panels except for **D`**-**F`** where anterior is to the left). Expression of head patterning genes in heat shock-treated WT (**A**, **D**, **D`**, **G**, **J**, **M**) and *hsp68-Tc-foxQ2* (**B**, **C**, **E**, **E`**, **F**, **F`**, **H**, **I**, **K**, **L**, **N**, **O**) embryos (14-18 h AEL) was monitored by ISH. (**B**, **C**) Ectopic *Tc-foxQ2* expression led to reduced *Tc-rx* expression. (**E**,**F**) *Tc-six4* expression showed a premature onset at the anterior tip (arrows) (compare embryonic stages of **E`**, **F`** with **D`**). Further, this premature expression was expanded. Further, an additional *Tc-six4* expression domain emerged more posterior (black arrowheads). (**H**, **I**) The *Tc-scro/nk2.1* expression started prematurely and was expanded. (**K**, **L**) In contrast, early elongating germ bands showed a reduced *Tc-scro/nk2.1* expression. This later effect was presumably a secondary effect. (**N**, **O**) The

anterior *Tc-cnc* expression domain spread towards posterior (empty arrowheads). The mandibular *Tc-cnc* expression domain was reduced and became somewhat spotty (open arrows).

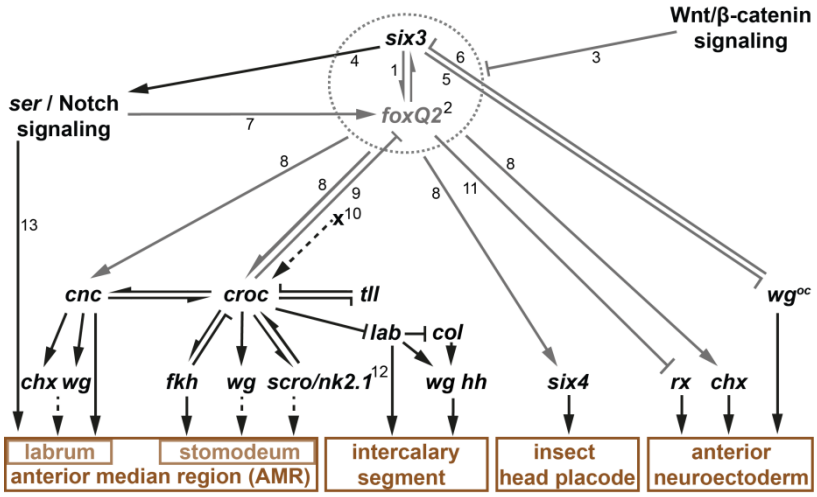

Fig. 10. *Tc-foxQ2* and *Tc-six3* form a regulatory module in the aGRN. Black lines indicate previously reported interactions (Based on (Kittelmann et al., 2013; Posnien et al., 2011c; Schaeper et al., 2010; Siemanowski et al., 2015)). Arrows represent gene activation, and cross-bars gene repression. This aGRN represents the interactions at early embryonic stages – later interactions are likely to differ. (**1**) *Tc-six3* is the most upstream factor for patterning the anterior median head and neuroectoderm. (**2**) *Tc-foxQ2*, like *Tc-six3*, is a key player in anterior head development with a somewhat later onset of expression than *Tc-six3*. Mutual activation, similar effects on other genes and similar phenotypes suggest that they form a regulatory module (indicated by the dashed circle). (**3**) *Tc-foxQ2* and *Tc-six3* are both antagonized by Wnt/β-catenin signaling. (**4**) *Tc-six3* acts on Notch signaling via *Tc-ser*. (**5/6**) Mutual repression of *Tc-six3* and the ocular *Tc-wg* expression. (**7**) Notch signaling-dependent activation of *Tc-foxQ2* is restricted to lateral parts of the anterior *Tc-foxQ2* expression. (**8**) Regulatory activity of *Tc-foxQ2* and *Tc-six3* is similar with respect to several downstream targets. (**9**) *Tc-foxQ2* but not *Tc-six3* is repressed by *Tc-croc* activity. (**10**) An unknown factor '*X*' is predicted to activate the posterior part of the *Tc-croc* expression, while *Tc-six3* and *Tc-foxQ2* are required for the anterior portion. (**11**) *Tc-rx* is repressed by *Tc-foxQ2* but is not regulated by *Tc-six3*. Note that the assumed repressive effect is based on non-overlapping expression of these genes and the effects found in misexpression experiments (see text for conflicting RNAi data). (**12**) The late effect of *Tc-foxQ2* on *Tc-scro/nk2.1*, observed in gain-of-function experiments, is most likely secondary and is, hence, not

considered here. (**13**) Notch signaling is involved in labrum development by regulating cell proliferation.

Supplementary Material

Supplementary Figures

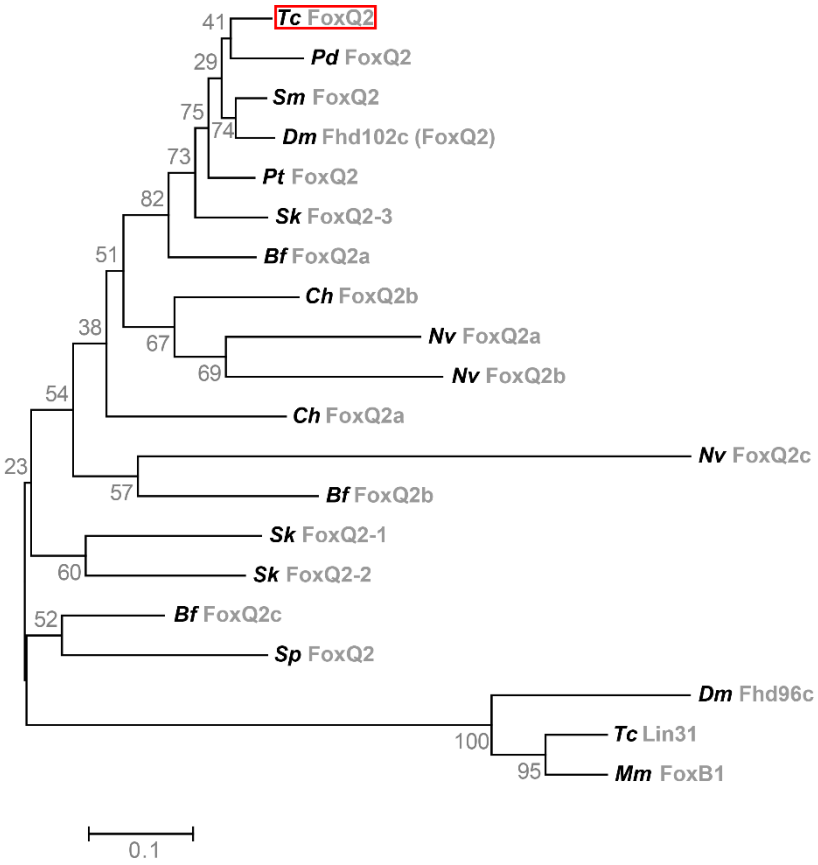

Fig. S1. Phylogenetic tree of FoxQ2 proteins within the Metazoa. *Tc-foxQ2* encodes for a FoxQ2 protein, which clusters together with the protostome orthologs. The closest protein sequence in the *Tribolium* genome (Tc-Lin31) is clearly outside the *foxQ2* clade showing that there is only one *Tribolium foxQ2* gene. Shown is a Neighbor-Joining tree with bootstrap values (grey numbers). Analysis of the same alignment using Maximum likelihood led to similar relationships. *Tc: Tribolium castaneum, Pd: Platynereis dumerilii, Sm: Strigamia maritima, Dm: Drosophila melanogaster, Pt: Parasteatoda tepidariorum, Sk: Saccoglossus kowalevskii, Nv: Nematostella vectensis, Ch: Clytia hemisphaerica, Bf: Branchiostoma floridae, Sp: Strongylocentrotus purpuratus, Mm: Mus musculus*.

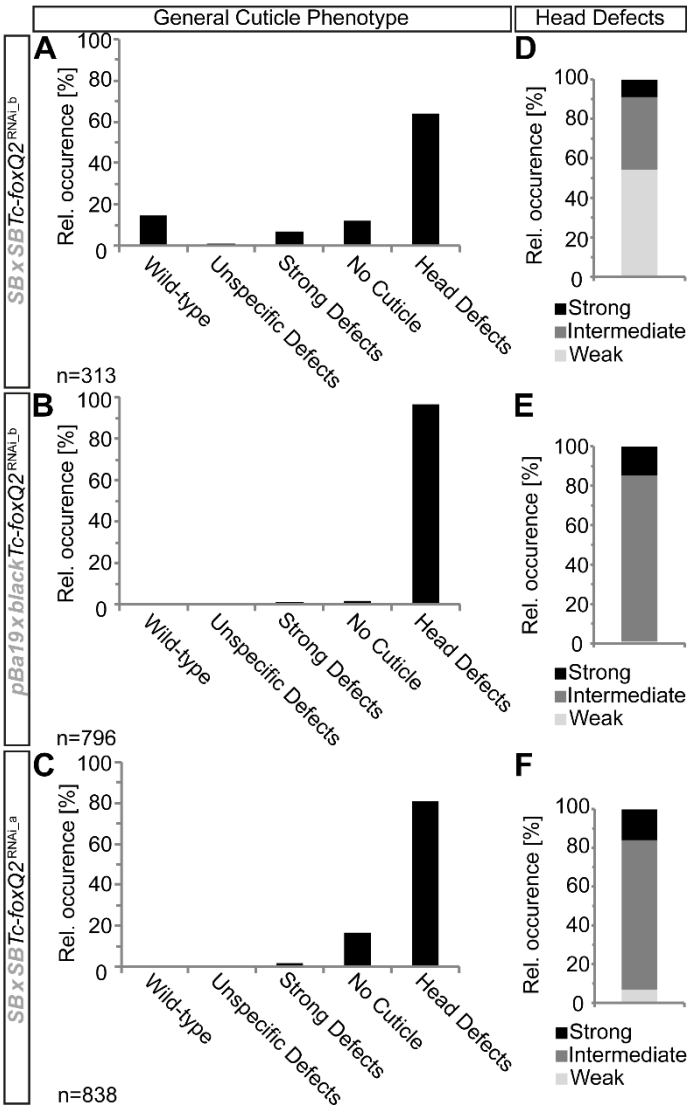

Fig. S2. Quantitative analysis of the *Tc-foxQ2*^{RNAi} epidermal L1 phenotypes in two different strains shows no considerable strain-specific effects. (**A,B**) Knockdown of *Tc-foxQ2* using the *Tc-foxQ2*$^{RNAi\_b}$ dsRNA fragment in the *SB* strain leads to a distribution of L1 larval cuticle phenotypes (A), which is comparable to the distribution of phenotypes in L1 offspring, when the same dsRNA fragment is injected in pupal *pig19* females, which were crossed to *black* males (B). (**B,C**) The distribution of the general phenotype classes gets even more similar when compared to the RNAi experiment using the *Tc-foxQ2*$^{RNAi\_a}$ dsRNA fragment in the *SB* strain (compare C and B). (**D-F**) Likewise, the frequency and quality of head defects is comparable throughout the RNAi experiments in different genetic backgrounds. (Data from A, D, C, F taken from Fig. 1)

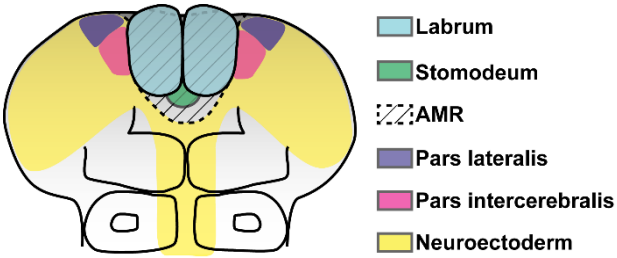

Fig. S3. Overview of the location of the most relevant embryonic head structures for this study. Anterior is up. The anterior median region (AMR, striped region) harbors the labral buds (blue) and the stomodeum (mouth precursor, green). This region is enframed by the neuroectoderm (yellow), in which the central neuroendocrine centers pars lateralis (purple) and pars intercerebralis (pink) are located (Velasco 2007). (Based on Posnien 2010, Kittelmann 2013)

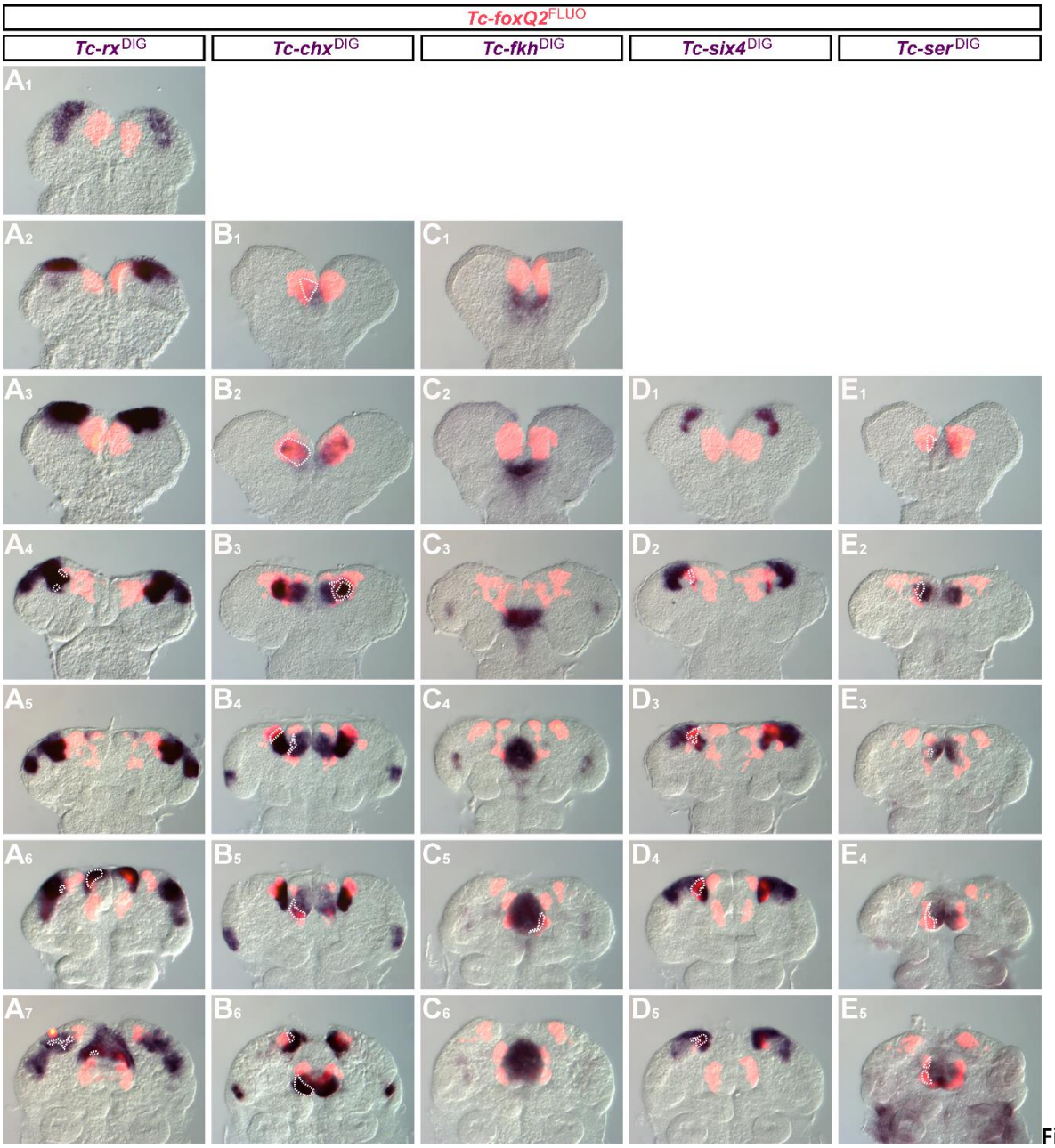

Fig. S4. Co-expression analyses of *Tc-foxQ2* and anterior head patterning genes II. Anterior is up. Expression is visualized by double ISH, using TSA-Dylight550 (red) and NBT/BCIP (blue). Co-expression is indicated with dashed lines. (**A**$_{0\text{-}6}$) *Tc-rx* is not co-expressed with *Tc-foxQ2* until fully elongated germ band stages (**A**$_{0\text{-}4}$), except for two little spots in the neurogenic region in late elongating germ bands (**A**$_3$). In retracting germ bands both genes are partially overlapping within the neurogenic region and in anterior parts of the labral buds (**A**$_5$, **A**$_6$). (**B**$_{0\text{-}5}$) *Tc-chx* expression is partially (**B**$_0$) and later almost completely (**B**$_1$) overlapping with *Tc-foxQ2* expression. At later stages the co-expression is restricted to narrow stripes within the outer lateral labral and the neurogenic region (**B**$_{2,}$ **B**$_3$). In early retracting germ bands *Tc-chx* expression shows only a little overlap within the posterior portion of the labral buds (**B**$_4$) and at later stages an additional overlap within the neurogenic region (**B**$_5$).

(**C**$_{0\text{-}5}$) *Tc-fkh* shows almost no co-expression with *Tc-foxQ2*, except for a small domain in the stomodeal region, in early retracting germ bands (**C**$_5$). (**D**$_{0\text{-}4}$) *Tc-six4* is not co-expressed with *Tc-foxQ2*, in intermediate elongating germ bands (**D**$_0$). Co-expression starts in late elongating germ bands and is restricted to a domain within the neurogenic region throughout the depicted stages (**D**$_{1\text{-}4}$). (**E**$_{0\text{-}1}$) *Tc-ser* is partially co-expressed with *Tc-foxQ2* within a small sub-region of the AMR at elongating germ band stages (**E**$_{0\text{-}1}$). (**E**$_{2\text{-}4}$) At later stages the co-expression is restricted to outer lateral parts of the labral buds.

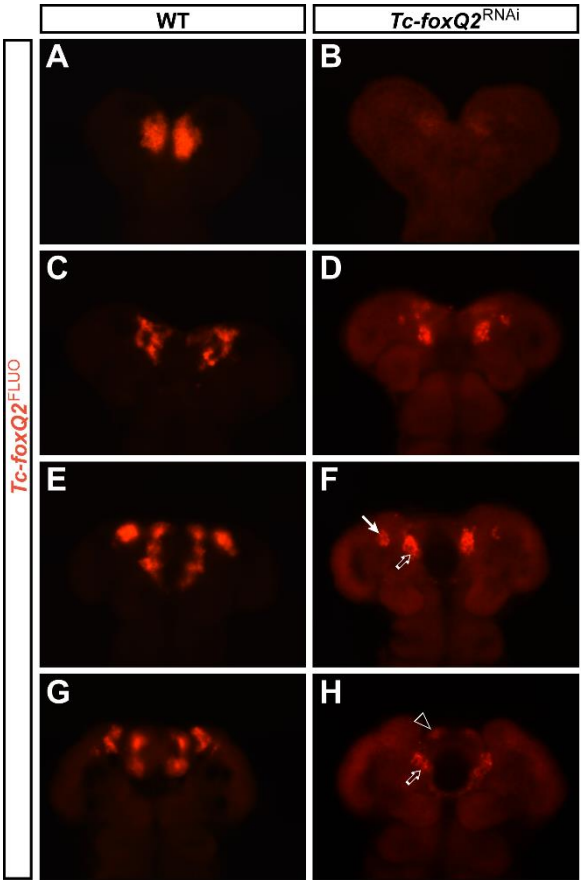

Fig. S5. Endogenous *Tc-foxQ2* mRNA is not completely abolished after *Tc-foxQ2* RNAi. Anterior is up. Expression of *Tc-foxQ2* in WT (**A,C,E,G**) and *Tc-foxQ2*^{RNAi} (**B,D,F,H**) embryos is monitored by ISH. Shown are *Tc-foxQ2*^{RNAi} embryos with typical staining. Note that the exposure time had to be strongly increased to detect residual staining (see elevated background in B,D,F,H). (B) *Tc-foxQ2* expression is almost completely deleted upon RNAi treatment of early elongating germ bands. (D) In *Tc-foxQ2*^{RNAi} late elongating germ bands the posterior portion of the *Tc-foxQ2* expression is still detectable. (F) Fully elongated germ band stages show expression in the neurogenic region (arrow) and the stomodeal flanking region (empty arrow). (H) In early retracting *Tc-foxQ2*^{RNAi} embryos *Tc-foxQ2* expression is detectable in the anterior part of the labral buds (empty arrowhead) and the stomodeal region (empty arrow).

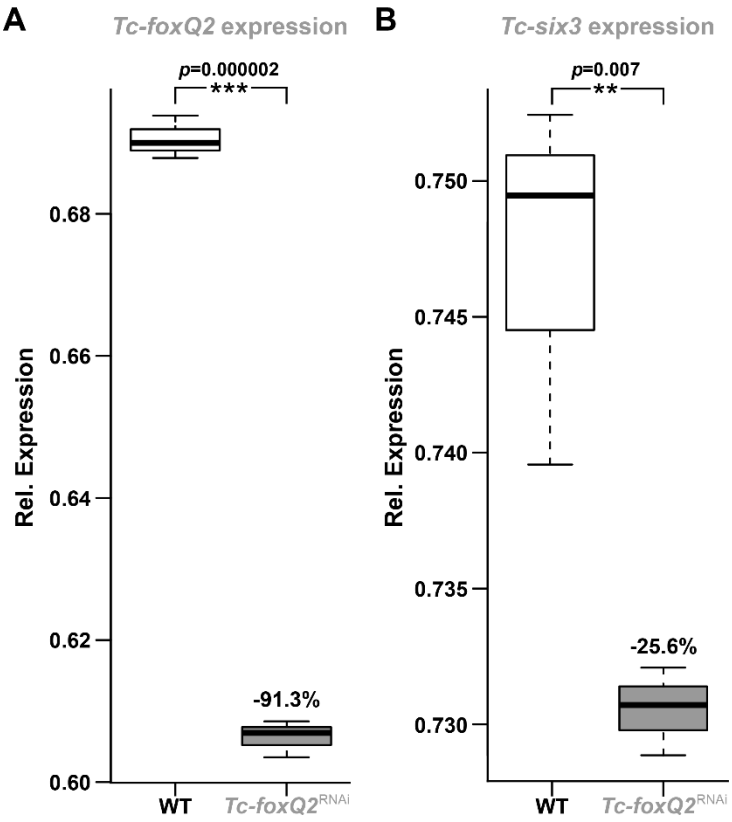

Fig. S6. *Tc-six3* and *Tc-foxQ2* expression are reduced in early *Tc-foxQ2*^{RNAi} embryos.

Box plots depicting relative expression levels of *Tc-foxQ2* (**A**) and *Tc-six3* (**B**) in WT and *Tc-foxQ2*^{RNAi} embryos at early stages (9-15 h AEL). (A) *Tc-foxQ2* expression is efficiently knocked down ($\mathbf{2}^{-\Delta\Delta CT}$: -91.3% ± 0.96) by RNAi using the *Tc-foxQ2*$^{RNAi\_a}$ dsRNA fragment. (B) *Tc-six3* expression is decreased ($\mathbf{2}^{-\Delta\Delta CT}$: -25.6% ± 0.05) after *Tc-foxQ2* RNAi. For further details, see the supplementary Material and Methods. The line inside the box represents the median, the box is defined by the first and the third quartile, the whiskers are defined by still being within 1.5 IQR of the lower/upper quartile.

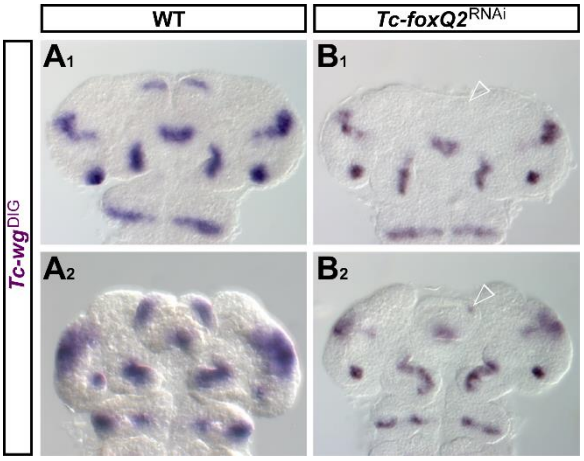

Fig. S7. *Tc-foxQ2*^{RNAi} embryos show a reduction of the labral *Tc-wg* expression domains. Anterior is up. Expression of *Tc-wg* in WT (**A_{1-2}**) and *Tc-foxQ2*^{RNAi} (**B_{1-2}**) embryos is monitored by ISH. (B_{1-2}) *Tc-wg* expression within the labral region is completely absent (B_1: empty arrowhead) or strongly reduced (B_2: empty arrowhead), after *Tc-foxQ2* RNAi.

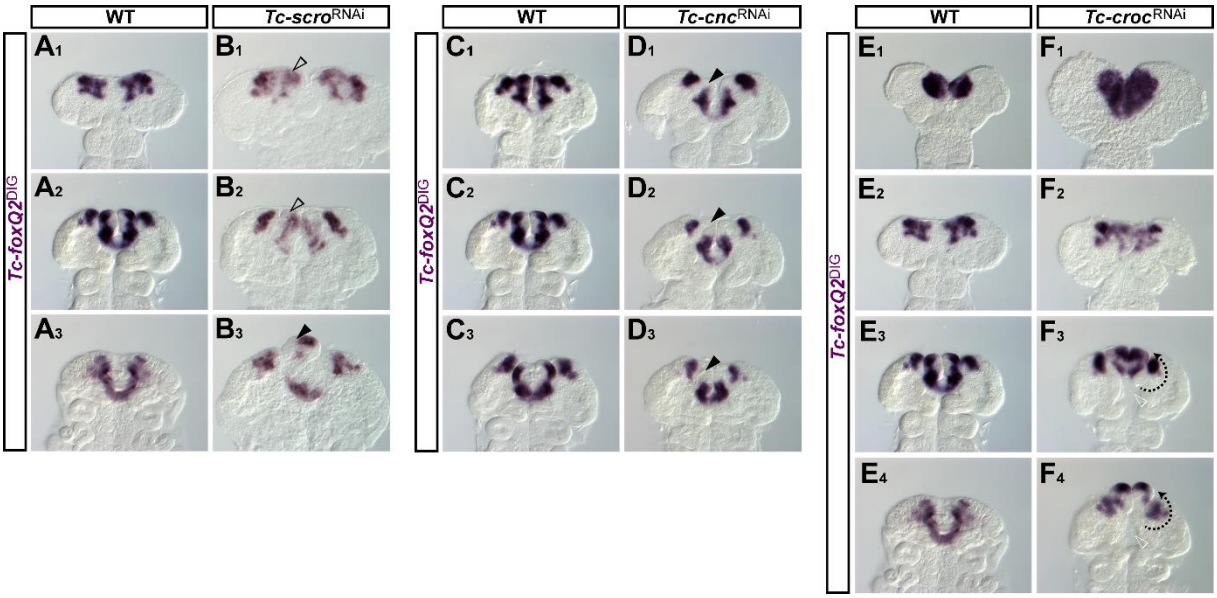

Fig. S8. Late *Tc-foxQ2* expression in *Tc-scro/nk2.1*^{RNAi}, *Tc-cnc*^{RNAi}, and *Tc-croc*^{RNAi}. Anterior is up. Expression of *Tc-foxQ2* in WT (**A**$_{1-3}$, **C**$_{1-3}$, **E**$_{1-4}$), *Tc-scro/nk2.1*^{RNAi} (**B**$_{1-3}$), *Tc-cnc*^{RNAi} (**D**$_{1-3}$), and *Tc-croc*^{RNAi} (**F**$_{1-4}$) embryos. (B$_1$) *Tc-scro/nk2.1*^{RNAi} embryos show a slightly distorted *Tc-foxQ2* expression pattern at late elongating germ band stages within the prospective labral/stomodeal region (empty arrowhead). Prior to this stage no considerable expression alteration was observable. (B$_2$) Fully elongated germ bands show a residual labral *Tc-foxQ2* expression domain, which appears to be misplaced (empty arrowhead). (B$_3$) Retracting *Tc-scro/nk2.1*^{RNAi} germ bands show a *Tc-foxQ2* expression, which appears to be altered mainly due to a disarrangement of the labral buds (arrowhead). (D$_{1-3}$) Late *Tc-cnc*^{RNAi} embryos show no *Tc-foxQ2* expression within the labral buds, probably caused by an RNAi-induced loss of tissue (arrowhead). Prior to the depicted stages no considerable expression alteration was observable. (F$_1$) *Tc-croc*^{RNAi} embryos show, in early elongating germ bands, a posterior expansion of the *Tc-foxQ2* expression. The embryo appears larger due to a preparation artifact. Prior to this stage no considerable expression alteration was observable. (F$_2$) In late elongating embryos *Tc-foxQ2* expression was reduced and disarranged. (F$_{3-4}$) Posterior medial expression is lost (empty arrowheads), and due to the misplacement of the labral buds (indicated by dashed arrows) the expression appears additionally altered.

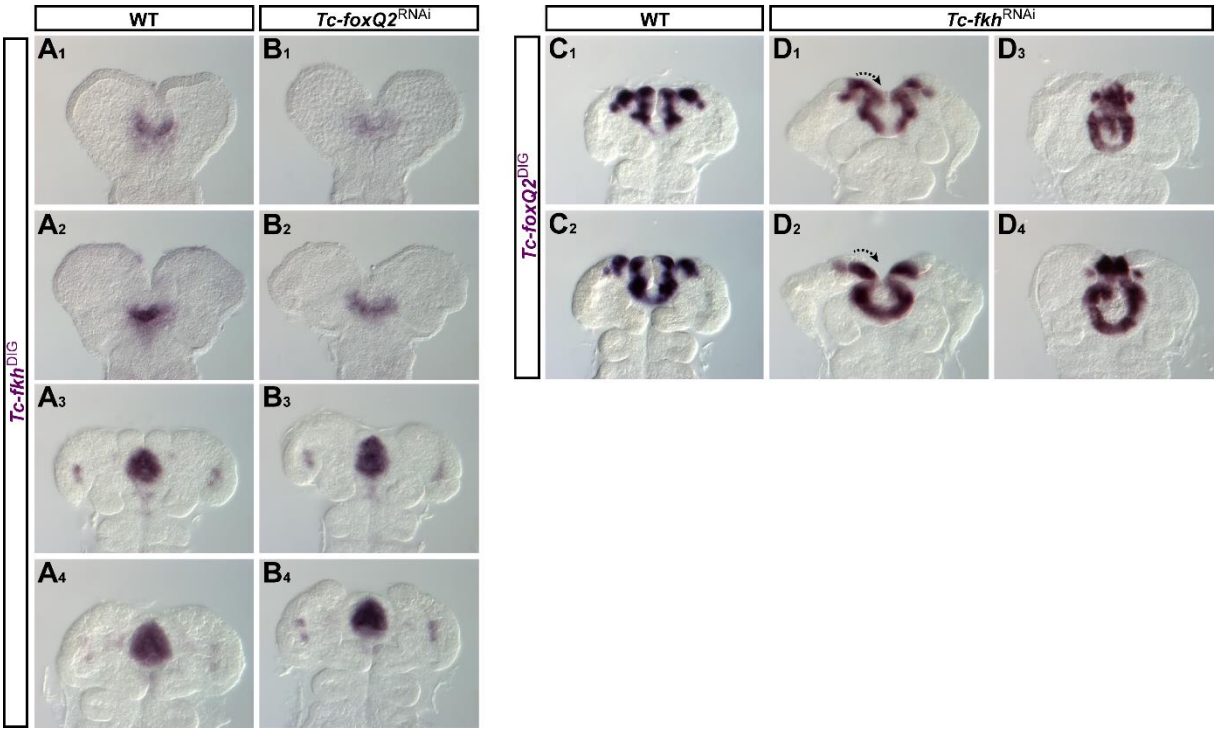

Fig. S9. No early interaction between *Tc-foxQ2* and *Tc-fkh*. Anterior is up. Expression of *Tc-fkh* in WT (**A$_{1-4}$**) and *Tc-foxQ2*^{RNAi} (**B$_{1-4}$**) embryos as well as expression of *Tc-foxQ2* in WT (**C$_{1-2}$**) and *Tc-fkh*^{RNAi} (**D$_{1-4}$**) embryos. (B$_{1-4}$) *Tc-foxQ2*^{RNAi} embryos show no considerably altered *Tc-fkh* expression throughout development. (D$_{1-4}$) Fully elongated *Tc-fkh*^{RNAi} embryos show an altered *Tc-foxQ2* expression pattern, which is probably a secondary effect caused by a moderate (D$_{1-2}$) or strong (D$_{3-4}$) turning of the antero-lateral head tissue towards the embryonic midline (D$_{1-2}$: turning indicated by dashed arrows).

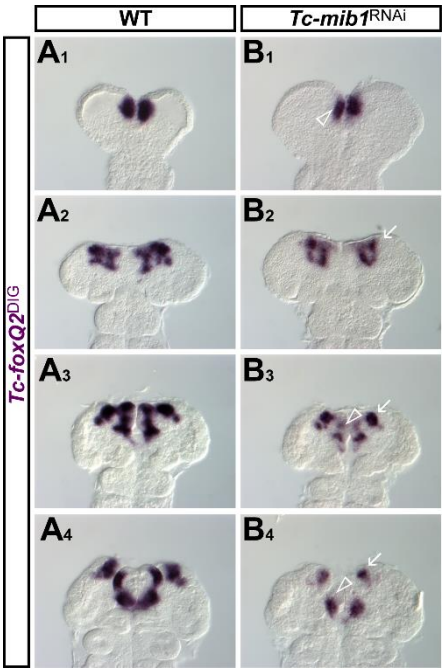

Fig. S10. *Tc-mib1*^{RNAi} embryos show altered *Tc-foxQ2* expression profile. Anterior is up. Expression of *Tc-foxQ2* in WT (**A_{1-4}**) and *Tc-mib1*^{RNAi} (**B_{1-4}**) embryos. (B_1) Early elongating *Tc-mib1*^{RNAi} embryos show medially reduced *Tc-foxQ2* expression domains (empty arrowhead). Prior to this stage no considerable alteration was observed. (B_2) In late elongating *Tc-mib1*^{RNAi} embryos the neurogenic part of the *Tc-foxQ2* expression was reduced (arrow). (B_{3-4}) Later stages show a reduction of the neurogenic expression domains (arrow) and a reduction of the anterior portion of the labral bud domains (empty arrowhead). The latter effect is most likely due to a loss of tissue caused by *Tc-mib1* RNAi.

Fig. S11. *Tc-six4* and *Tc-chx* but not *Tc-rx* regulate late *Tc-foxQ2* expression. Anterior is up. Expression of *Tc-foxQ2* in WT (**A_{1-5}**, **C_{1-3}**, **E_{1-3}**), *Tc-six4*^{RNAi} (**B_{1-5}**), *Tc-chx*^{RNAi} (**D_{1-3}**), and *Tc-rx*^{RNAi} (**F_{1-3}**) embryos. (B_{1-5}) *Tc-six4*^{RNAi} embryos show a reduction of the neurogenic *Tc-foxQ2* expression domains (arrows) at late stages. Prior to the depicted stages no considerable expression alteration was observable. (D_{1-3}) Late elongating to retracting *Tc-chx*^{RNAi} germ bands show an expansion of the neurogenic *Tc-foxQ2* expression domains (arrows), which leads to a fusion with the stomodeal expression domain. Prior these stages no considerable expression alteration was observable. (**F_{1-3}**) In *Tc-rx*^{RNAi} embryos no considerable change of the *Tc-foxQ2* expression pattern was detectable.

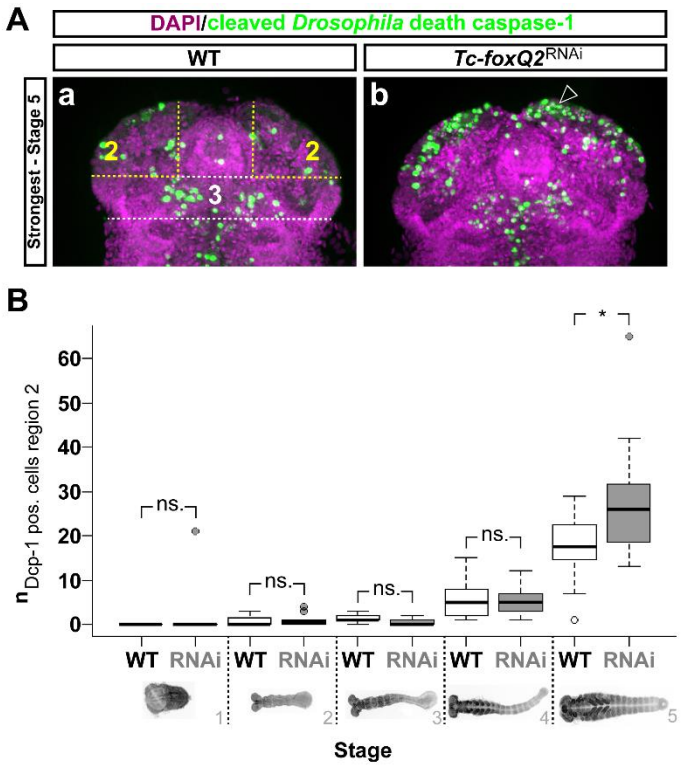

Fig. S12. Analysis of cell death rates within the neurogenic head region in *Tc-foxQ2*^{RNAi} embryos. Anterior is up (**A$_a$**, **A$_b$**). Apoptotic cells are, in WT (**A$_a$**) and in *Tc-foxQ2*^{RNAi} (**A$_b$**) embryos monitored by antibody staining (Dcp-1 – Alexa Fluor 488, green). Nuclei are stained (DAPI, magenta) to visualize the embryonic morphology. (A$_a$,A$_b$) Retracting germ bands with the highest number of apoptotic cells in WT (A$_a$) and *Tc-foxQ2*^{RNAi} (A$_b$) embryos. Indicated are the neurogenic region (ROI 2, yellow dashed lines) and the region, which was used for normalization of the data set (region 2, white dashed lines). The *Tc-foxQ2*^{RNAi} retracting germ band shows a strong accumulation of apoptotic cells within the neurogenic region (ROI 2). (B) Box plot depicting the number of apoptotic cells (y-axis) versus five different embryonic stages, subdivided in untreated and RNAi embryos (x-axis). The ROI 2 values are normalized with the region 3 values. Brackets display grade of significance. Germ rudiments (stage 1) to fully elongated germ bands (stage 4) show no significant increase of apoptotic cells within the ROI 2 (stage 1: p=0.33 (WT: n=3, RNAi: n=7), stage 2: p=0.35 (WT: n=11, RNAi: n=12), stage 3: p=0.99 (WT: n=9, RNAi: n=19), stage 4: p=0.23 (WT: n=17, RNAi: n=15)). However, retracting germ bands showed in the ROI 2 significantly more apoptotic cells (p=0.023) in RNAi embryos (n=11) compared to untreated embryos (n=12). The line inside the box represents the median, the box is defined by the first and the third quartile, the whiskers are defined by still being within 1.5 IQR of the lower/upper quartile. ns.: not significant

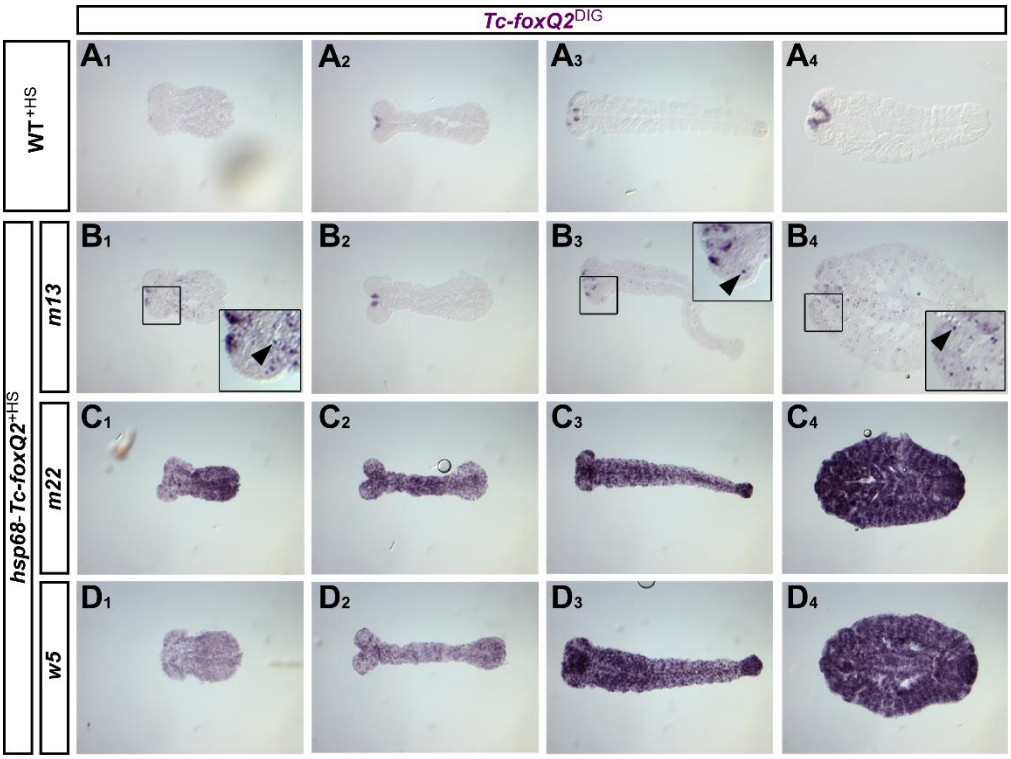

Fig. S13. Heat shock-induced *Tc-foxQ2* expression. Anterior is left. Expression of *Tc-foxQ2* in heat shock-treated WT (**A_{1-4}**), *hsp68-Tc-foxQ2$_{m13}$* (**B_{1-4}**), *hsp68-Tc-foxQ2$_{m22}$* (**C_{1-4}**) and *hsp68-Tc-foxQ2$_{w5}$* (**D_{1-4}**) embryos is monitored by ISH. (A_{1-4}) WT embryos show no change in the *Tc-foxQ2* expression pattern, upon heat shock treatment. (B_{1-4}) Individuals of the transgenic line *hsp68-Tc-foxQ2$_{m13}$* show ectopic *Tc-foxQ2* expression in some cells, which are scattered sparsely across embryo (boxes, arrowheads). (C_{1-4},D_{1-4}) Individuals of the transgenic lines *hsp68-Tc-foxQ2$_{m22}$* and *hsp68-Tc-foxQ2$_{w5}$* show a strong activation of ectopic *Tc-foxQ2* expression throughout the embryo. For the following experiments the line *hsp68-Tc-foxQ2$_{w5}$* was used, because of the more even distribution of ectopic *Tc-foxQ2* expression (D_{1-4}).

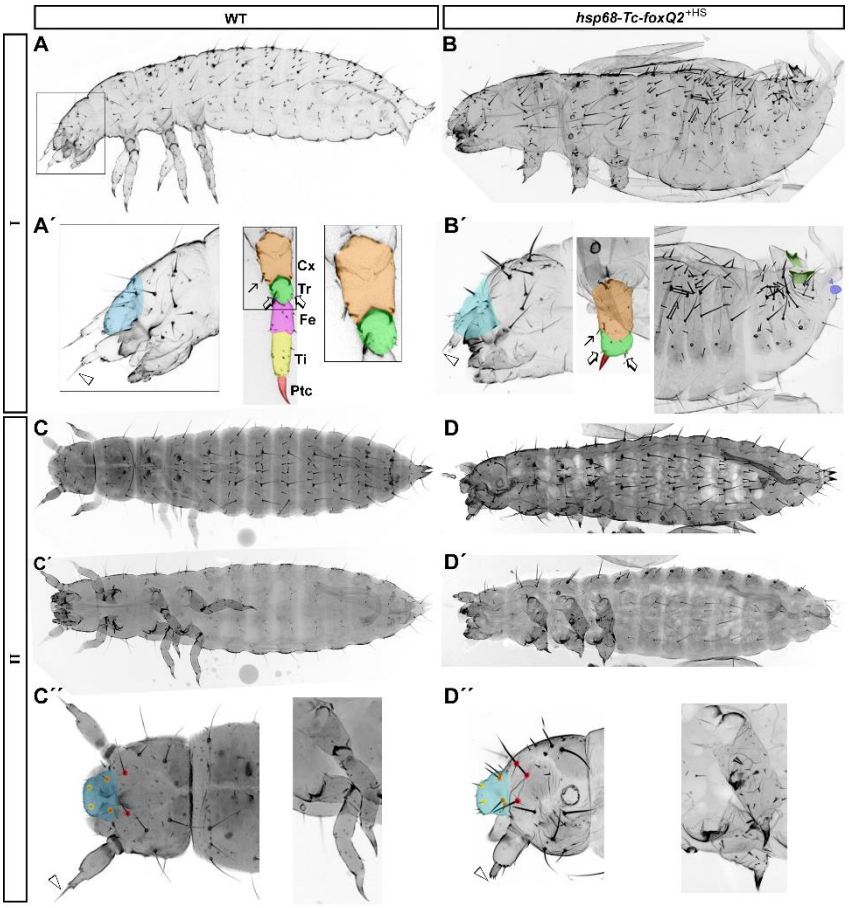

Fig. S14. Heat shock-induced *Tc-foxQ2* expression results in defects in L1 larval cuticles. Anterior is left. WT (**A,A`,C-C``**) and heat shock-treated *hsp68-Tc-foxQ2* (**B,B`,D-D``**) L1 larval cuticles, grouped into two classes (I and II). (B,B`) Embryonic *Tc-foxQ2* gain-of-function L1 cuticles, of the first phenotype class (I; >50% of the cuticles), showed an absence of the antennal flagellum (arrowhead) and a slightly disrupted bristle pattern (B` left panel). The legs (middle panel) had a reduced number of podomeres. Presumably, only the coxa (orange), trochanter (green) and the pre-tarsal claw (red) were left (compare bristles marked by arrows in A` and B`). The abdominal segments (right panel) were reduced in number and the remaining segments were dorsally fused. The urogomphi (green, here duplicated) and pygopods (blue, here reduced) were sometimes affected, as well. (D-D`) Embryonic *Tc-foxQ2* gain-of-function L1 cuticles, of the second phenotype class (II; approximately 30% of the cuticles), showed defects restricted to the head and thoracic region. (D``) A larval head (left panel) of the second phenotype class showing an absent antennal flagellum (arrowhead) and affected head appendages. The head bristle pattern was disrupted and showed frequently a duplication of the clypeus setae (orange dots) and the anterior vertex setae (red dots). The legs (right panel) showed comparable defects as the legs of the first phenotype class. Cx: coxa, Tr: trochanter, Fe: femur, Ti: tibia, Ptc: pre-tarsal claw

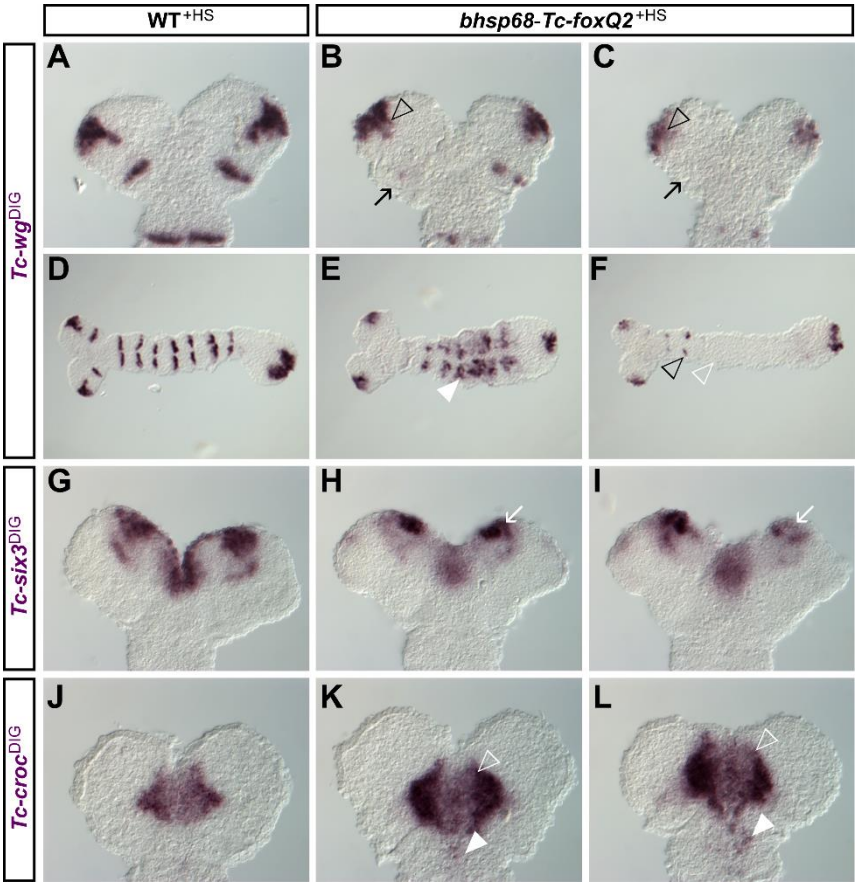

Fig. S15. Ectopic *Tc-foxQ2* expression impacts head patterning gene expression profiles II. Anterior is up (left in D-F)**.** Expression of head marker genes in heat shock-treated WT (**A,D,G,J**) and *hsp68-Tc-foxQ2* (**B,C,E,F,H,I,K,L**) embryos (14-18 h AEL) is monitored by ISH. (B,C) The ocular *Tc-wg* expression domain is slightly (B) or heavily (C) reduced (empty arrowheads), upon ectopic *Tc-foxQ2* expression. The antennal expression domains are heavily reduced (B: arrow) or completely absent (C: arrow). (E,F) The *Tc-wg* stripes posterior to the procephalon were collapsed (E: white arrowhead), reduced (F: black empty arrow) or completely absent (F: white arrowhead), in *hsp68-Tc-foxQ2*$^{+HS}$ embryos. (H,I) The neurogenic *Tc-six3* expression domains are reduced in *hsp68-Tc-foxQ2*$^{+HS}$ embryos (arrows). This contrasts with the early activation we found by RNAi but in line with later mutually exclusive expression of these genes. Note that heat shock-induced misexpression starts only at late blastoderm stages such that we were probably not able to recover the earliest interactions of the aGRN. (K,L) The *Tc-croc* expression pattern appears to be slightly expanded (empty arrowheads) and posteriorly spread (arrowheads), after ectopic *Tc-foxQ2* expression in line with the activating role found in RNAi experiments.

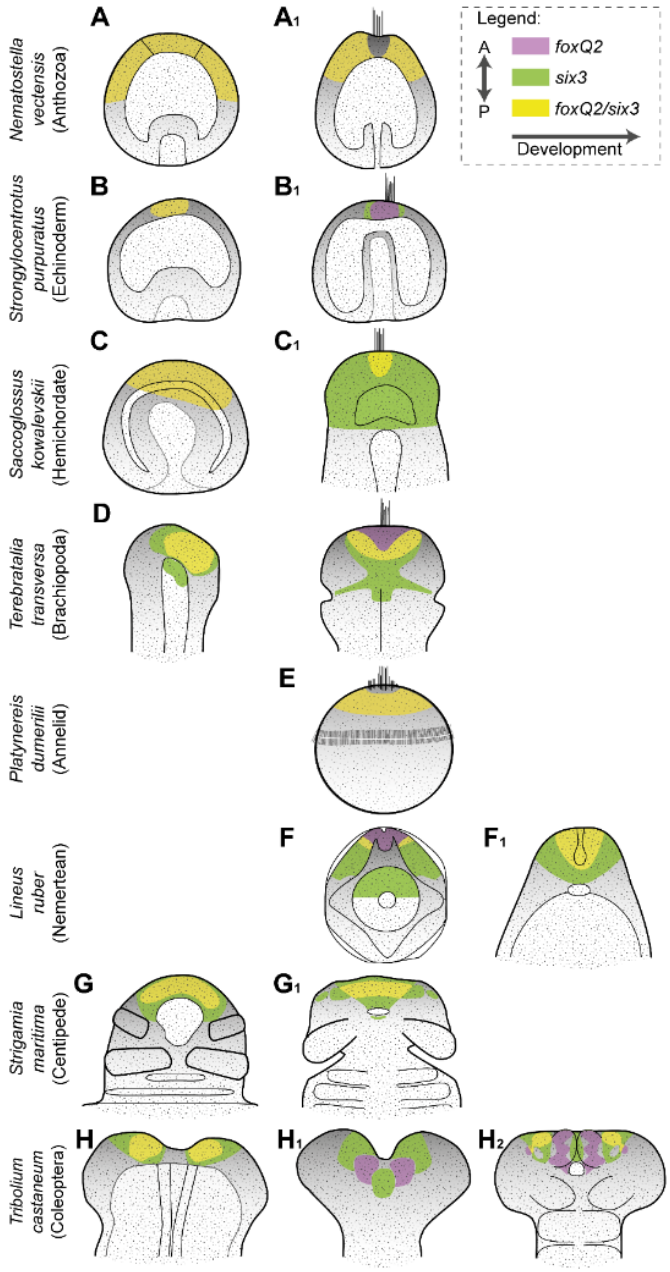

Fig. S16. Expression of *foxQ2*/*six3* orthologs in different Metazoa. *foxQ2* (purple) and *six3* (green) and their co-expression (yellow) at different developmental stages. The anterior/apical pole is oriented to the top. At early stages, co-expression of *foxQ2* and *six3* at the anterior pole of different metazoan species is highly conserved (left column). At later stages the patterns diverge leading to mutual exclusive expression in some taxa. (**A_1**, **E**) *Nematostella* and *Platynereis* larvae show a *foxQ2*/*six3* co-expression during early stages like the other species, with the exception that the most apical region is free of *foxQ2*/*six3* expression. (**C_1**, **F_1**, **G_1**) Late embryonic stages of *Saccoglossus* and *Strigamia* as well as early *Lineus* juveniles show a *foxQ2* expression at the anterior/apical pole, which is completely covered by *six3* expression. (**B_1**, **H_1**) *Strongylocentrotus* late gastrulae and *Tribolium* elongating germ bands show mutually exclusive expression of *foxQ2* and *six3* at later stages. (**D_1**, **F_1**) Early tri-lobed *Terebratalia* larvae and *Lineus* Schmidt's larvae show *foxQ2* expression at the anterior/apical pole overlapping only posteriorly with *six3*. (**$H_{2\text{-}3}$**) Fully elongated and retracting *Tribolium* germ bands show a complex expression pattern of *foxQ2* and *six3* with partial overlaps in the neuroectoderm (**$H_{2\text{-}3}$**) and in the anterior labral buds (**H_3**). (Based on (Fritzenwanker et al., 2014; Hunnekuhl and Akam, 2014; Marlow et al., 2014; Martín-Durán et al., 2015; Santagata et al., 2012; Sinigaglia et al., 2013; Tu et al., 2006; Wei et al., 2009); A: anterior, P: posterior

Supplementary Tables

Table S1. *Tc-foxQ2*$^{RNAi\_a}$ general cuticle phenotype using 1 µg/µl dsRNA in *SB*.

Phenotype:	Wildtype	Unspecific defects	Strong defects	No cuticle	Head defects	Total n
∑	4	0	18	140	676	838
%	0.5	0	2.1	16.7	80.7	

Table S2. *Tc-foxQ2*$^{RNAi\_b}$ general cuticle phenotype using 1 µg/µl dsRNA in *SB*.

Phenotype:	Wildtype	Unspecific defects	Strong defects	No cuticle	Head defects	Total n
∑	47	4	23	39	200	313
%	15	1.3	7.3	12.5	63.9	

Table S3. *Tc-foxQ2*$^{RNAi\_a}$ head defects using 1 µg/µl dsRNA in *SB*.

Phenotype:	Weak	Intermediate	Strong
∑	47	522	107
%	7	77.2	15.8

Table S4. *Tc-foxQ2*$^{RNAi\_b}$ head defects using 1 µg/µl dsRNA in *SB*.

Phenotype:	Weak	Intermediate	Strong
∑	109	73	18
%	54.5	36.5	9

Table S5. *Tc-foxQ2*$^{RNAi\_b}$ general cuticle phenotype using 1 µg/µl dsRNA in *SB*.

Phenotype:	Wildtype	Unspecific defects	Strong defects	No cuticle	Head defects	Total n
∑	47	4	23	39	200	313
%	15	1.3	7.3	12.5	63.9	

Table S6. *Tc-foxQ2*$^{RNAi\_b}$ head defects using 1 µg/µl dsRNA in *SB*.

Phenotype:	Weak	Intermediate	Strong
∑	109	73	18
%	54.5	36.5	9

Tables S7 & S8.

Click here to Download Tables S7 and S8

Supplementary Material and Methods

RT-qPCR

Total RNA was isolated from eggs (9-15 h AEL) using TRIzol® reagent (Invitrogen™, Schwerte, Germany). Isolated RNA was treated with TURBO DNA-free™ Kit (Invitrogen™, Schwerte, Germany). cDNA was synthesized by using the Maxima® First Strand cDNA Synthesis Kit for RT-qPCR (Thermo Scientific™, Schwerte, Germany). qPCR was performed using HOT FIREpol® EvaGreen® qPCR Mix Plus (ROX) (Solis BioDyne, Tartu, Estonia) and the CFX96™ Real-Time PCR Detection System (Bio-Rad Laboratories, München, Germany). All primers were designed to span an intronic sequence and were validated by gel analysis (For primer sequences see Table S8.). Each sample was performed in technical and biological triplicates. To calculate primer efficiency ($E=10^{(-1/m)}$), a dilution series was performed. Relative concentrations of mRNA were normalized to ribosomal protein *Tc-rps18* (Lord 2010) C_t. For statistical analysis, Student's t-Test was performed. Fold changes were calculated using the $\mathbf{2}^{-\Delta\Delta CT}$ -method (Schmittgen and Livak, 2008).